

RELIEF: Reinforcement Learning Empowered Graph Feature Prompt Tuning

Jiapeng Zhu
East China Normal University
Shanghai, China
jiapengzhu@stu.ecnu.edu.cn

Zichen Ding
East China Normal University
Shanghai, China
zichending@stu.ecnu.edu.cn

Jianxiang Yu
East China Normal University
Shanghai, China
jianxiangyu@stu.ecnu.edu.cn

Jiaqi Tan
East China Normal University
Shanghai, China
jiaqitan@stu.ecnu.edu.cn

Xiang Li*
East China Normal University
Shanghai, China
xiangli@dase.ecnu.edu.cn

Weining Qian
East China Normal University
Shanghai, China
wnqian@dase.ecnu.edu.cn

ABSTRACT

The advent of the “pre-train, prompt” paradigm has recently extended its generalization ability and data efficiency to graph representation learning, following its achievements in Natural Language Processing (NLP). Initial graph prompt tuning approaches tailored specialized prompting functions for Graph Neural Network (GNN) models pre-trained with specific strategies, such as edge prediction, thus limiting their applicability. In contrast, another pioneering line of research has explored universal prompting via adding prompts to the input graph’s feature space, thereby removing the reliance on specific pre-training strategies. However, the necessity to add feature prompts to all nodes remains an open question. Motivated by findings from prompt tuning research in the NLP domain, which suggest that highly capable pre-trained models need less conditioning signal to achieve desired behaviors, we advocate for strategically incorporating necessary and lightweight feature prompts to certain graph nodes to enhance downstream task performance. This introduces a combinatorial optimization problem, requiring a policy to decide 1) which nodes to prompt and 2) what specific feature prompts to attach. We then address the problem by framing the prompt incorporation process as a sequential decision-making problem and propose our method, RELIEF, which employs Reinforcement Learning (RL) to optimize it. At each step, the RL agent selects a node (discrete action) and determines the prompt content (continuous action), aiming to maximize cumulative performance gain. Extensive experiments on graph and node-level tasks with various pre-training strategies in few-shot scenarios demonstrate that our RELIEF outperforms fine-tuning and other prompt-based approaches in classification performance and data efficiency. The code is available at <https://github.com/JasonZhujp/RELIEF>.

*Corresponding author

Permission to make digital or hard copies of all or part of this work for personal or classroom use is granted without fee provided that copies are not made or distributed for profit or commercial advantage and that copies bear this notice and the full citation on the first page. Copyrights for components of this work owned by others than the author(s) must be honored. Abstracting with credit is permitted. To copy otherwise, or republish, to post on servers or to redistribute to lists, requires prior specific permission and/or a fee. Request permissions from [permissions@acm.org](https://www.acm.org).
Conference acronym 'XX, June 03–05, 2018, Woodstock, NY
© 2018 Copyright held by the owner/author(s). Publication rights licensed to ACM.
ACM ISBN 978-1-4503-XXXX-X/18/06
<https://doi.org/XXXXXXX.XXXXXXX>

CCS CONCEPTS

• **Information systems** → **Data mining**; • **Computing methodologies** → **Knowledge representation and reasoning**; **Reinforcement learning**.

KEYWORDS

Graph neural networks, prompt tuning, reinforcement learning, hybrid action space, few-shot learning

ACM Reference Format:

Jiapeng Zhu, Zichen Ding, Jianxiang Yu, Jiaqi Tan, Xiang Li, and Weining Qian. 2018. RELIEF: Reinforcement Learning Empowered Graph Feature Prompt Tuning. In *Proceedings of Make sure to enter the correct conference title from your rights confirmation email (Conference acronym 'XX)*. ACM, New York, NY, USA, 17 pages. <https://doi.org/XXXXXXX.XXXXXXX>

1 INTRODUCTION

In recent years, Graph Neural Networks (GNNs) have been applied in diverse domains, including knowledge graphs [23], social networks [2], and recommender systems [15], due to their powerful expressivity in capturing complex relationships in real-world data. However, traditional supervised learning on graphs struggles with limited labeled data and poor generalization to out-of-distribution samples [49]. To overcome these challenges, significant efforts have focused on pre-trained GNN models [43, 45], which are first trained on label-free graphs in a self-supervised manner to learn intrinsic properties, followed by fine-tuning on downstream tasks.

Despite advancements, the “pre-train, fine-tune” paradigm still exhibits drawbacks. The misalignment between pre-training and downstream objectives can lead to sub-optimal performance, known as negative transfer [9]. Moreover, under few-shot settings, pre-trained models are prone to overfitting, leading to catastrophic forgetting [24], which compromises their generalization ability. To tackle the issues, prompt learning, which has shown remarkable success in Natural Language Processing (NLP) [1, 21, 25] and Computer Vision (CV) [13, 17, 48], emerges as a promising approach. By designing informative prompts to manipulate input data, prompt tuning aligns objectives between pretext and downstream tasks, thereby augmenting the potential of pre-trained models.

Naturally, researchers have extended the “pre-train, prompt” framework to graph domain [38]. Existing approaches are broadly divided into two categories based on whether they depend on pre-training strategies. For methods reliant on pre-training strategies,

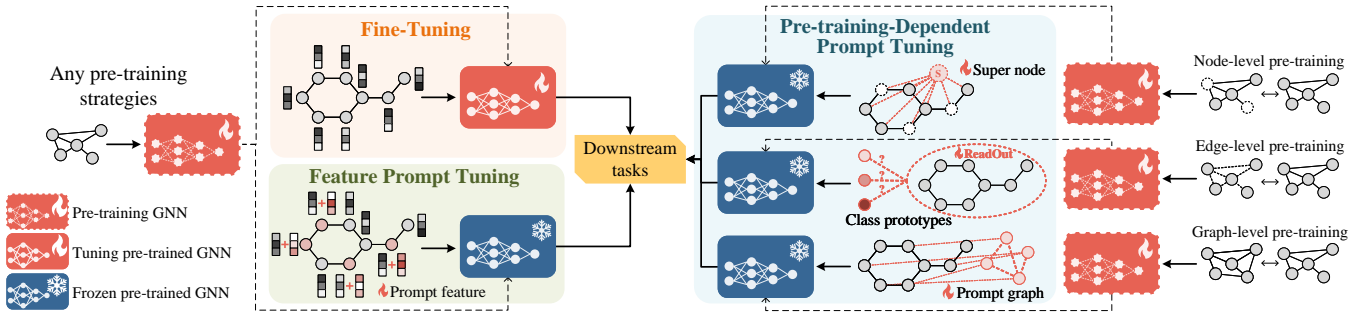


Figure 1: A Comparison of Tuning Methods. Fine-tuning (upper left) updates the parameters of the pre-trained GNN model. Pre-training-dependent prompt tuning (right) freezes the GNN model and requires designing specialized prompt templates aligned with pre-training strategies, whereas feature prompt tuning (lower left) is applicable to any pre-training strategy.

GPPT [35] and GraphPrompt [26] unify pretext and downstream tasks as edge prediction. All in One [37] introduces a prompt graph to match the graph-level contrastive learning used in pre-training. SGL-PT [53] aligns the downstream task with masked node prediction using contrastive and generative learning objectives. However, these methods may fail if a GNN model is pre-trained with multiple self-supervised techniques through multi-task learning to enhance model’s capabilities, rather than solely simple link prediction.

In contrast, prompting methods agnostic to pre-training strategies offer greater compatibility. GPF [5], a pioneering method in this line, introduces graph feature-based prompt tuning, demonstrating that adding a learnable uniform feature prompt vector to each node is theoretically equivalent to any graph manipulation, without restricting pre-training strategies. GPF-plus [5], a variant of GPF, provides more flexible adaptation by inserting node-specific prompted features. SUPT [20], a subsequent study, innovated by assigning feature prompts at the subgraph level, captures intricate contextual nuances of each subgraph, leading to a decent performance improvement. Thus, feature-based prompting forms the basis of our paper due to its generality and effectiveness.

Nonetheless, it is critical to delve deeper into existing feature-based prompting methods. In NLP, soft prompt tuning adapts frozen language models for specific tasks using continuous prompt tokens [25]. Research shows that while increasing prompt token length involves more tunable parameters and thus enhances expressivity, excessively long prefixes can degrade test performance [22, 52]. In fact, T5-XXL can achieve strong results even with a single-token prompt, indicating that more capable models need less conditioning signal to exhibit desired behavior [21]. This finding is even more enlightening in the context of graphs. Since most GNNs follow the message-passing mechanism, information from a feature prompt attached to a target node will propagate to its neighbors, diffusing the influence of prompting signals to a broader range.

We propose that given an adequately pre-trained GNN model, judiciously inserting minimal prompts as conditioning signals may suffice for downstream tasks. In the realm of feature prompting, “minimal” can be translated as an appropriate amount and magnitude of prompts. Conversely, incorporating prompts to an excessive number of nodes increases learnable parameters, raising the risk of overfitting [22], particularly with few-shot downstream data.

Moreover, since prompts are directly added to node features, large-magnitude prompts might overwhelm the original input’s feature space, causing pre-trained GNNs to perceive prompted graphs as unfamiliar, leading to a decline in transfer performance.

Hence, the key lies in **strategically incorporating necessary and lightweight prompts into the original graph**, allowing a GNN model to fully leverage its learned knowledge during pre-training without being overly disrupted, and to better generalize to downstream tasks through flexible feature prompts.

The choice of prompting on certain nodes and attaching specific feature prompts leads to a combinatorial optimization problem. To tackle this, we turn to Reinforcement Learning (RL), which effectively searches for heuristic strategies by training an agent [28], and propose a **RE**inforcement **L**earn**I**ng **E**mpowered graph **F**eature prompting method, named RELIEF. We formulate the process of inserting prompts as a sequential decision-making problem. At each step, the RL agent: 1) selects which node to prompt (discrete action), and 2) determines the prompt content, i.e., specific values of the prompt vector (continuous action). Therefore, an RL algorithm capable of handling the discrete-continuous hybrid action space [4, 27, 46] is employed. The prompted graph is then evaluated by the pre-trained GNN model. At the subsequent step, a new prompt generated by the RL agent is added to the previous prompted graph. Prompt addition and performance evaluation are repeated until a maximum step is reached. Our goal is to maximize the expected cumulative performance gain on the downstream task. Techniques like policy generalization [7, 30, 41] are integrated to ensure training stability and effectiveness. Furthermore, we have designed two metrics: *prompt coverage ratio* and *average prompt magnitude* to quantify the extent to which the prompt affects the original input.

Our contributions are summarized as follows:

- We suggest enhancing the performance of pre-trained GNN models on downstream tasks by adding necessary and lightweight feature prompts and design metrics to quantify their impact on inputs, offering a new perspective on graph prompt tuning.
- As far as we know, we are the first to formulate feature prompt incorporation as a sequential decision-making problem, and propose RELIEF, an RL empowered graph feature prompting method optimized through trial and error in a hybrid action space.

- Extensive experiments across both graph and node-level tasks with various pre-training strategies in few-shot scenarios demonstrate that RELIEF achieves superior classification performance and data efficiency compared to fine-tuning and other competitive prompt-based methods.

2 PRELIMINARIES

Let an undirected graph instance be $\mathcal{G} = (\mathcal{V}, \mathcal{E}, \mathbf{X}) \in \mathbb{G}$, where $\mathcal{V} = \{v_1, v_2, \dots, v_n\}$ denotes the node set containing n nodes; $\mathcal{E} = \{(v_i, v_j) \mid v_i, v_j \in \mathcal{V}\}$ denotes the edge set; $\mathbf{X} = \{x_1, x_2, \dots, x_n\} \in \mathbb{R}^{n \times D}$ denotes the node feature matrix, where $x_i \in \mathbb{R}^{1 \times D}$ is the feature vector of node v_i with feature dimension D . The adjacency matrix $\mathbf{A} \in \{0, 1\}^{n \times n}$ is defined such that $\mathbf{A}_{ij} = 1$ if $(v_i, v_j) \in \mathcal{E}$.

Fine-tuning and Graph Prompt Tuning. Given a pre-trained GNN model f_θ and a task-specific projection head g_ϕ for making predictions, parameters θ and ϕ are fine-tuned on a downstream training dataset $\mathcal{D} = \{(\mathcal{G}_1, y_1), \dots, (\mathcal{G}_m, y_m)\}$ to maximize the likelihood of correctly predicting label y of graph \mathcal{G} , described as:

$$\max_{\theta, \phi} \prod_{i=0}^m P_{f_\theta, g_\phi}(y_i \mid \mathcal{G}_i) = \max_{\theta, \phi} \prod_{i=0}^m g_\phi(f_\theta(\mathbf{X}, \mathbf{A})) [y_i]$$

where $[y_i]$ fetches the prediction probability of label y_i from $g_\phi(\cdot)$. In contrast, the pre-trained GNN model f_θ remains frozen during prompt tuning. The primary focus shifts to learning a prompting function $u_\psi : \mathbb{G} \rightarrow \mathbb{G}$, which transforms the original graphs \mathcal{G} to prompted graphs $u_\psi(\mathcal{G})$, used as inputs to the GNN model. The projection head g_ϕ is also tuned to coordinate with the prompting function. The optimal u_ψ and g_ϕ are obtained by:

$$\max_{\psi, \phi} \prod_{i=0}^m P_{f_\theta, g_\phi}(y_i \mid u_\psi(\mathcal{G}_i)) = \max_{\psi, \phi} \prod_{i=0}^m g_\phi(f_\theta(\mathbf{X}_\psi, \mathbf{A}_\psi)) [y_i]$$

where \mathbf{X}_ψ and \mathbf{A}_ψ are prompted feature and adjacency matrix, respectively, acquired by prompting function u_ψ . For evaluation, the downstream testing graphs are first transformed by the prompting function and then passed through the pre-trained GNN model, followed by the projection head to produce predictions.

Graph Feature Prompt Tuning. This line of prompting method introduces learnable components to the feature space of the input graph. Given the node feature matrix $\mathbf{X} = \{x_1, x_2, \dots, x_n\}$ of a graph \mathcal{G} , learnable prompt feature vectors $p_1, p_2, \dots, p_n \in \mathbb{R}^{1 \times D}$ are added to node features. This can be viewed as the prompting function u_ψ , achieving a prompted feature matrix \mathbf{X}^* expressed as:

$$\mathbf{X}^* = \{x_1 + p_1, x_2 + p_2, \dots, x_n + p_n\} = \{x_1^*, x_2^*, \dots, x_n^*\}$$

and \mathbf{X}^* is then processed by the GNN model. Note that feature prompt tuning does not explicitly prompt on the adjacency matrix, thus the representation of a prompted graph is given by $f_\theta(\mathcal{G}^*) = f_\theta(\mathbf{X}^*, \mathbf{A})$. Different feature prompting methods vary in their prompt vector designs or learning approaches. A comparison of aforementioned tuning methods is depicted in Figure 1.

RL with Hybrid Action Space. Most RL algorithms operate within either discrete or continuous action spaces [39]. In our scenario, however, we deal with a hybrid action space [27, 46], involving selecting nodes (discrete) and specifying feature prompts (continuous). Formally, discrete actions are chosen from a finite set

$\mathcal{A}_d = \{a_1, a_2, \dots, a_n\}$, each corresponding to a real-valued continuous action $z \in \mathbb{R}^D$, where D is the dimension of the continuous action space $\mathcal{A}_c = \{z_1, z_2, \dots, z_n\}$. H-PPO [4] is an RL algorithm tailored for hybrid action spaces based on actor-critic architecture. It employs two parallel actor networks for discrete and continuous actions, respectively, alongside a single critic network for value estimation. H-PPO extends Proximal Policy Optimization (PPO) [33] by separately optimizing the two actors with an entropy-regularized PPO surrogate objective \mathcal{L}^{PPO} to maximize expected cumulative discounted reward, while the critic minimizes Mean Squared Error (MSE) loss $\mathcal{L}^{\text{Critic}}$ to improve value estimation accuracy. For a detailed introduction to PPO and H-PPO, please refer to Appendix E.

3 METHOD

In this section, we first introduce the formulation of a Markov Decision Process (MDP) designed for our feature prompting scenario (Section 3.1). We then detail the architecture of the policy network to instantiate the MDP (Section 3.2). Next, we present the overall framework of RELIEF, featuring alternating training (Section 3.3). To mitigate policy overfitting, we integrate policy generalization techniques (Section 3.4). Additionally, we describe two metrics designed to quantify the impact of the inserted feature prompts on original graphs (Section 3.5). Note that we use graph-level classification as an example throughout this section and will later extend to node tasks in the experiments section.

3.1 Incorporating Feature Prompts as MDP

In RL domain, the environment is typically modeled by an MDP [39]. With the aim of framing the process of incorporating prompts as an MDP, we present the design of the basic elements as follows.

Action Space. Given a graph \mathcal{G} with n nodes, a discrete action a is to select a node v_a from the node set $\{v_1, \dots, v_n\}$, and a continuous action $z \in \mathbb{R}^{1 \times D}$ is to determine a real-valued vector for node v_a , where D is the dimension of the initial node feature. Thus, a hybrid action, i.e., feature prompt, incorporated at time step t can be denoted as $(a_t, z_t) = p_t^{a, z}$. We further define the prompt matrix at step t as $\mathbf{P}_t = \{p_{1,t}, \dots, p_{n,t}\} \in \mathbb{R}^{n \times D}$. \mathbf{P}_0 is initialized as a zero matrix, indicating no prompt is applied. Thus, the prompted feature \mathbf{X}^* of a prompted graph \mathcal{G}^* is obtained by $\mathbf{X}^* = \mathbf{X} + \mathbf{P}$.

State Transition. We define the state space as node representations of the prompted graph \mathcal{G}^* obtained from the pre-trained GNN model f_θ . This allows the agent to be aware of node representations that closely tied to the GNN model, enabling precise control. Formally, the state at time step t is denoted as:

$$\begin{aligned} s_t &:= f_\theta(\mathcal{G}_{t-1}^*) = f_\theta(\mathbf{X}_{t-1}^*, \mathbf{A}) = f_\theta(\mathbf{X} + \mathbf{P}_{t-1}, \mathbf{A}) \\ &= \{h_{1,t-1}^*, \dots, h_{n,t-1}^*\} \in \mathbb{R}^{n \times d} \end{aligned}$$

where $h_{i,t-1}^*$ is the representation of node v_i in the prompted graph \mathcal{G}_{t-1}^* , and d is the dimension of the latent space. Notably, the current state builds upon the representation of the previous step. However, as different graphs contain varying numbers of nodes, this results in state spaces of different sizes, posing challenges for batch training. To fix the size, we set a maximum number of nodes N and use zero padding, i.e., append $(N - n)$ zero vectors $\mathbf{0} \in \mathbb{R}^{1 \times d}$ to the end of

$h_{n,t}^*$, ensuring a fixed-size state representation:

$$\begin{aligned} s_t &:= f_\theta(\mathbf{X}_{t-1}^*, \mathbf{A}) \parallel \mathbf{0}_{(N-n) \times d} \\ &= \{h_{1,t-1}^*, \dots, h_{n,t-1}^*, \mathbf{0}_{n+1}, \dots, \mathbf{0}_N\} \in \mathbb{R}^{N \times d} \end{aligned} \quad (1)$$

where \parallel denotes concatenation. When the agent executes action $p_t^{a,z}$ at step t , which inherently operates on node v_a 's feature prompt p_a , the prompted feature matrix then transits to $\mathbf{X}_t^* = \mathbf{X} + \mathbf{P}_t$, with \mathbf{P}_t computed as:

$$\mathbf{P}_t = \mathbf{P}_{t-1} + p_t^{a,z} = \{p_{1,t-1}, \dots, p_{a,t-1} + p_t^{a,z}, \dots, p_{n,t-1}\}$$

Finally, the next state s_{t+1} is obtained by replacing \mathbf{X}_{t-1}^* in Eq. (1) with \mathbf{X}_t^* . Practically, this involves feeding the prompted graph \mathcal{G}_t^* into the pre-trained GNN model to derive new node representations, along with zero padding, to construct the subsequent state.

Reward Function. An ideal reward function is goal-oriented, providing guiding signals about action values during exploration. While downstream task metrics such as AUC or F1-score might seem straightforward for graph classification tasks, we require a reward to measure the quality of prompt inserted at each step for each graph. However, these metrics are infeasible to apply to a single graph. Instead, we use the loss decrease as our instant reward, since it captures the concept of performance gain somewhat and can be derived from each graph. Formally, given two adjacent steps, the reward $r(s_t, a_t, z_t, s_{t+1})$, or r_t for short, is defined as:

$$r_t = \mathcal{L}_{t-1} - \mathcal{L}_t = \mathcal{L}(g_\phi(f_\theta(\mathcal{G}_{t-1}^*)), y) - \mathcal{L}(g_\phi(f_\theta(\mathcal{G}_t^*)), y) \quad (2)$$

where $\mathcal{L}(\cdot)$ denotes a loss function associated with the downstream task, such as cross-entropy loss for classification. Hence, the reward is positive if the prompt assigned at this step leads to a loss decrease, and negative if it increases loss. Consequently, the cumulative reward reflects the total loss decrease from time step 1 to T , serving as a surrogate measurement of overall performance improvement.

3.2 Policy Network Architecture

RELIEF employs H-PPO, comprising two parallel actor networks and a single critic network collectively referred to as the policy network Π_ω , where ω denotes the parameters of these networks.

In practice, all the three networks share the first few layers to encode state information. Since the state space is designed as the node representations of a prompted graph, we utilize the pre-trained GNN model f_θ as the state encoder. Thereafter, Multi-Layer Perceptrons (MLPs) with different output dimensions are connected to each of the three networks, facilitating the corresponding functions. Given a prompted graph \mathcal{G}^* , the forward propagation of the networks is presented as follows:

$$\begin{aligned} p(a | s) &\leftarrow \text{SOFTMAX}(\text{MLP}_a(f_\theta(\mathcal{G}^*))) \\ \boldsymbol{\mu}(s, a) &\leftarrow \text{MLP}_z(f_\theta(\mathcal{G}^*)) [a] \\ V(s) &\leftarrow \text{MLP}_c(\text{FLATTEN}(f_\theta(\mathcal{G}^*))) \end{aligned}$$

Let's elaborate on each expression in turn.

Discrete Actor. Represents the discrete policy $\pi_d(a|s)$. Given node representations of a prompted graph as state s , i.e., $f_\theta(\mathcal{G}^*)$ with size $N \times d$, the MLP_a followed by a SOFTMAX operation transforms s into a discrete action probability $p(a|s) \in \mathbb{R}^n$. The agent then either samples a node v_a based on this probability or greedily

selects the node with the highest probability as a discrete action, indicating a stochastic or deterministic policy, respectively. Note that we set the entries in $p(a|s)$ associated with zero padding to zero, eliminating their chance of being selected, which reduces the number of valid discrete actions from N to n .

Continuous Actor. Represents the continuous policy $\pi_c(z|s, a)$. Given state $s \in \mathbb{R}^{N \times d}$, the MLP_z outputs N parameters $\boldsymbol{\mu} \in \mathbb{R}^{1 \times D}$ for all the N possible discrete actions. Then $\boldsymbol{\mu}$ with index $[a]$ is chosen paired with the selected discrete action a . Subsequently, the agent constructs a Gaussian distribution based on $(\boldsymbol{\mu}, \boldsymbol{\sigma})$ and samples a vector $z \in \mathbb{R}^{1 \times D}$ as a prompt feature $p^{a,z}$ stochastically, or directly use $\boldsymbol{\mu}$ as the action deterministically, where the standard deviation $\boldsymbol{\sigma} \in \mathbb{R}^{1 \times D}$ can either be learned or pre-defined. To ensure $p^{a,z}$ remains within a desired range, each dimension of z is clamped to range $[-z_{\max}, z_{\max}]$, where $z_{\max} > 0$ is a hyper-parameter controlling the scale of the prompt added at every step.

Critic. Used for estimating the state-value function. At its core, it maps a state s to a real value $V(s) \in \mathbb{R}$. However, there exists a dimension discrepancy: our state space possesses a node-level granularity, whereas value estimation is based on a global view. Therefore, we use FLATTEN operation to transform the size of state s from $N \times d$ to $1 \times Nd$. The flattened vector is then passed through MLP_c to produce a real value, treated as the estimation of $V(s)$.

It is worth noting that the state encoder in the policy network Π_ω is a direct copy of the pre-trained GNN model and keeps frozen during policy learning. This implies it is by updating the parameters of the MLPs, that the actors are enabled to map states to actions, and the critic is enabled to map states to state values. Such structure has been widely used in RL from Human Feedback (RLHF) practice [3, 29], where reward models and policy networks are constructed on fixed LLMs with learnable linear layers appended.

3.3 Overall Framework of RELIEF

RELIEF contains two trainable modules: the policy network and the projection head, as illustrated in Figure 2. Effective coordination of these two modules greatly enhances the prompting performance. We train them alternatively in practice, as described below.

3.3.1 Policy network training. Given the frozen pre-trained GNN model f_θ , the policy network Π_ω , the projection head g_ϕ and a graph \mathcal{G} with label y containing n nodes, the initial loss \mathcal{L}_0 is computed via $\mathcal{L}(g_\phi(f_\theta(\mathcal{G})), y)$, with no prompt attached.

At each step, the agent samples a feature prompt $p_t^{a,z}$ with respect to the policies π_d and π_c , and adds it to node v_a . The prompted graph is then passed to the GNN model followed by the projection head to obtain the current loss according to label y . By comparing the current loss with the previous one, an instant reward is computed by Eq. (2). As a result, the agent collects a transition, denoted as a tuple (s, a, z, r, s') . The prompt addition process is repeated n times, equivalent to the number of nodes, theoretically giving every node a chance of being prompted. Notably, both actors use stochastic policies for better exploration during training.

Next, the collected n transitions are used to update the policy network. The two actors are independently trained using the PPO surrogate objective \mathcal{L}^{PPO} , whereas the critic is trained by MSE loss

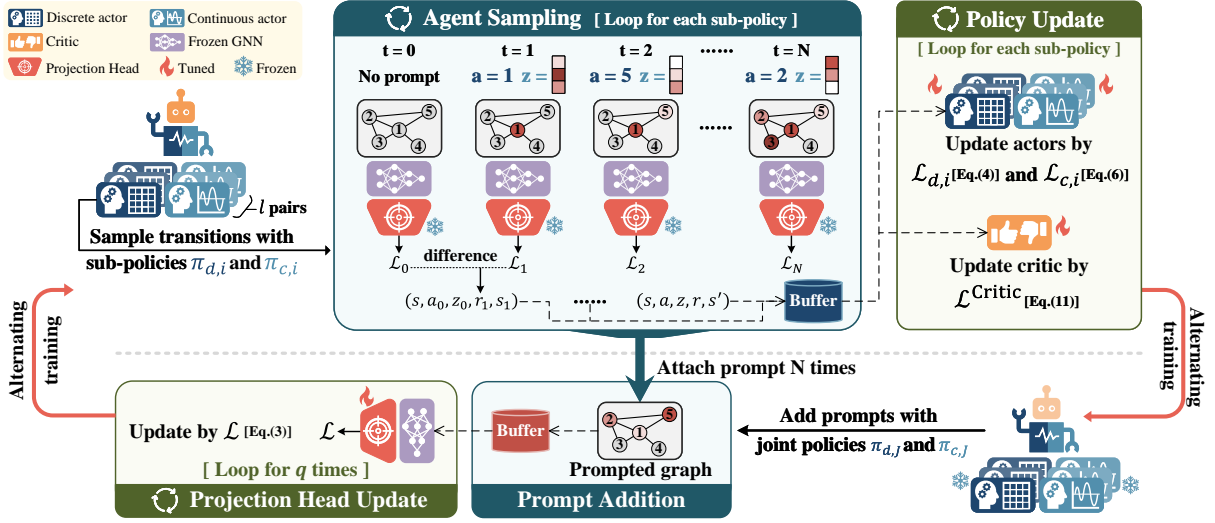


Figure 2: RELIEF pipeline. The policy network (upper) and the projection head (lower) are trained alternately. Feature prompts are incorporated during the agent sampling and prompt addition processes via discrete and continuous actors.

$\mathcal{L}^{\text{Critic}}$. The above process is batchified by consuming a batch of graphs simultaneously to increase sampling and training efficiency.

3.3.2 Projection head training. This aligns predictions with their correct labels by coordinating the projection head with representations of the ultimate prompted graphs. Thus, we use the learned policy to insert feature prompts for n steps to obtain the final prompted graph \mathcal{G}^* . Here, we modify the continuous policy to be deterministic, ensuring identical prompt vector values for the same state and discrete action. This guarantees stable prompted graphs and thus consistent representations, which together with the labels, are used to supervise the projection head update. Given m graph samples, the projection head g_ϕ is updated by minimizing the objective:

$$\min_{\phi} \frac{1}{m} \sum_{i=1}^m \mathcal{L}(g_\phi(f_\theta(\mathcal{G}_i^*)), y) \quad (3)$$

where $\mathcal{L}(\cdot)$ is the same loss function as in Eq. (2). To facilitate a more rapid coordination of the projection head with the policy, the projection head is updated q times.

To summarize, the above alternating process – training policy network once and projection head q times – defines a training epoch. At the evaluation stage, we directly apply the two learned actors to incorporate feature prompts step by step into the downstream validation and testing graphs. These prompted graphs are transformed by the pre-trained GNN model and the learned projection head to produce predictions, which are then measured by downstream metrics.

3.4 Policy Generalization

When trained in a limited set of environments, general RL algorithms often exhibit overfitting, resulting in poor generalization to unseen testing scenarios [30, 41], which is exactly the case in few-shot prompt tuning. To tackle this, we introduce a policy generalization technique, named LEEP [7], which can be seamlessly integrated with PPO, and thus compatible to our RELIEF.

Practically, LEEP is an ensemble-based method designed for discrete action spaces, adding a regularization term to PPO surrogate objective \mathcal{L}^{PPO} for updating the actor network. LEEP learns a generalized joint policy by leveraging all sub-policies. To generalize our discrete policy $\pi_d(a|s)$, we learn l discrete sub-policies $\{\pi_{d,1}, \dots, \pi_{d,l}\}$. Each $\pi_{d,i}$ gathers transitions from a training graph set \mathcal{D}_i , which is bootstrap-sampled from the entire training set \mathcal{D} . Each $\pi_{d,i}$ is updated by maximizing the expected reward, while minimizing the disagreement between $\pi_{d,i}$ itself and the joint discrete policy $\pi_{d,J}$, i.e., maximizing the following objective:

$$\mathcal{L}_{d,i} = \mathcal{L}_{d,i}^{\text{PPO}} - \alpha_d \mathbb{E}_{s \sim \pi_{d,i}, \mathcal{D}_i} \left[D_{\text{KL}}(\pi_{d,i}(a|s) || \pi_{d,J}(a|s)) \right] \quad (4)$$

where $\alpha_d > 0$ is a uniform penalty hyper-parameter for all discrete sub-policies and D_{KL} denotes the KL-divergence. The discrete joint policy $\pi_{d,J}$ combines all sub-policies $\pi_{d,i}$, and is computed as:

$$\pi_{d,J}(a|s) = \frac{\max_{i=1, \dots, l} \pi_{d,i}(a|s)}{\sum_{a'} \max_{i=1, \dots, l} \pi_{d,i}(a'|s)} \quad (5)$$

indicating that to obtain the discrete action probability $p(a|s)$ given by $\pi_{d,J}$, we take the maximum probability across all l sub-policies for each action a , and normalize these maxima by their sum across all actions.

Since RELIEF requires hybrid action spaces, we extend LEEP to continuous action spaces. Similarly, we learn l continuous sub-policies $\{\pi_{c,1}, \dots, \pi_{c,l}\}$, each exploring in its respective training contexts \mathcal{D}_i . In other words, we employ l parallel H-PPO algorithms, but still with a single critic. Each continuous sub-policy $\pi_{c,i}$ is trained by maximizing the following objective:

$$\mathcal{L}_{c,i} = \mathcal{L}_{c,i}^{\text{PPO}} - \alpha_c \mathbb{E}_{s \sim \pi_{c,i}, \mathcal{D}_i} \left[D_{\text{KL}}(\pi_{c,i}(a|s) || \pi_{c,J}(a|s)) \right] \quad (6)$$

where $\alpha_c > 0$ is a uniform penalty hyper-parameter for continuous sub-policies. The continuous joint policy $\pi_{c,J}$ is defined as:

$$\pi_{c,J}(z|s, a) = \frac{1}{l} \sum_{i=1}^l \pi_{c,i}(z|s, a) = \frac{1}{l} \sum_{i=1}^l \mu_i(s, a) \quad (7)$$

indicating that the average mean μ_i of all sub-policies is used as the continuous joint policy.

To sum up, the policy network, enhanced by policy generalization techniques, now comprises l discrete actors, l continuous actors and a single critic. During training, discrete and continuous actors within each pair are independently updated using Eq. (4) and (6), respectively, followed by the critic update using $\mathcal{L}^{\text{Critic}}$. Each pair of actors is sequentially updated. The joint policies $\pi_{d,J}$ and $\pi_{c,J}$ are applied to incorporate prompt features when training the projection head or testing at the evaluation stage. The pseudo-code for RELIEF can be found in Appendix F. Additionally, a detailed complexity analysis is in Appendix G.

3.5 Metrics for Quantifying Prompts Impact

Our RELIEF stands out from existing feature prompting methods [5, 20] by incorporating necessary and lightweight feature prompts. To measure the disturbance to the original input space caused by these prompts, we introduce two metrics: Prompt Coverage Ratio (PCR) and Average Prompt Magnitude (APM).

Prompt Coverage Ratio. Given a graph \mathcal{G} with n nodes, and the final prompt matrix $\mathbf{P} = \{p_1, \dots, p_n\} \in \mathbb{R}^{n \times D}$ obtained by adding feature prompts $p^{a,z}$ over n steps, starting from a zero matrix, PCR is calculated as:

$$\text{PCR}(\mathcal{G}) = \frac{1}{n} \sum_{i=1}^n \mathbf{1}[p_i \neq \mathbf{0}_{1 \times D}] \in [0, 1] \quad (8)$$

where $\mathbf{1}[\cdot]$ is the indicator function, which equals 1 if the feature prompt p_i is not a zero vector $\mathbf{0}_{1 \times D}$ (i.e., a valid prompt), otherwise 0. PCR signifies the proportion of nodes prompted at least once during the entire prompt addition process.

Average Prompt Magnitude. We use L1-norm of the valid feature prompts averaged over dimensions, to describe the magnitude of inserted prompts, which is computed as:

$$\text{APM}(\mathcal{G}) = \frac{1}{n} \sum_{i=1}^n \frac{1}{D} \mathbf{1}[p_i \neq \mathbf{0}_{1 \times D}] \cdot \|p_i\|_1 \in [0, +\infty) \quad (9)$$

where $\|p_i\|_1$ denotes the Manhattan norm of p_i , i.e., the sum of the absolute values of all entries of p_i . Thus, APM characterises the scale of valid feature prompts, offering a tangible measurement in terms of “lightweight”.

PCR and APM collectively assess how extensively and significantly feature prompts are integrated, which are applicable for evaluating any feature prompting methods.

4 RELATED WORK

4.1 Graph Prompt Tuning

Graph prompt tuning research can be categorized based on whether the prompting methods are independent of pre-training strategies. For methods paired with specific pre-trained GNN models, GPPT [35] and GraphPrompt [26] align pretext and downstream tasks using link prediction. All in One [37] unifies tasks at graph

level and incorporates learnable prompt graphs tuned by meta-learning. PSP [6] and Self-Pro [8] further adapt prompting approaches to heterophilous graphs by introducing graph-level dual-view and asymmetric contrastive learning, respectively, as pretext tasks, preserving more graph structural information.

Although these methods have shown success, their reliance on specific pre-training strategies limits their applicability. In contrast, feature prompt tuning, has demonstrated comparable results across various pre-training strategies. Pioneering works like GPF, GPF-plus [5], and SUPT [20] introduce learnable feature prompts to every node. However, they potentially overemphasize prompts and disrupt the input space, which may degrade performance.

To the best of our knowledge, our work is the first to apply RL to graph feature prompt tuning, aiming to optimize a policy for inserting necessary and lightweight feature prompts to enhance the downstream tasks performance of pre-trained GNN models.

4.2 RL for Graph Representation Learning

The integration of RL into graph representation learning has advanced significantly. MAG-GNN [18] uses DQN to select optimal subgraph subsets to achieve high expressivity. WSD [42] employs weighted sampling for subgraph counting, with edge weights determined by DDPG. SUGAR [36] preserves hierarchical graph properties by selecting subgraphs using an RL pooling mechanism based on Q-learning. GPA [10] utilizes DQN to learn optimal annotation strategies for valuable nodes in active search, while GraphCBAL [51] further employs A2C for a class-balanced active search strategy.

While these works typically apply basic RL algorithms to either select actions from finite sets or determine single real values, RELIEF employs RL in a hybrid action space, skillfully integrating policy generalization techniques to achieve intricate control, representing a more cohesive fusion of RL and graph learning.

5 EXPERIMENTS

5.1 Few-shot Graph Classification

GNN Architecture and Datasets. We use a 5-layer GIN [47] as the base architecture for the GNN model, which is pre-trained on chemistry datasets [11] and prompt tuned on molecule properties prediction benchmark from MoleculeNet [44] as downstream tasks, following the setup in existing feature prompting works [5, 20]. Detailed descriptions of these datasets are provided in Appendix B.1.

Pre-training Strategies. To demonstrate the generality of our RELIEF, we pre-train the GIN model with four common strategies at both node and graph levels: Deep Graph Infomax (Infomax) [40], Attribute Masking (AttrMasking) [11], Context Prediction (ContextPred) [11], and Graph Contrastive Learning (GCL) [50]. Detailed descriptions of these methods are available in Appendix B.2.

Baselines. We compare RELIEF with the following tuning approaches, all of which involve adjusting the projection head: additionally, **Fine-Tuning (FT)** tunes the parameters of the pre-trained GNN model; **feature prompt tuning methods**, including GPF, GPF-plus [5], SUPT_{soft} and SUPT_{hard} [20], tune the parameters of learnable feature prompts with the GNN model fixed; **other prompt-based method**, All in One [37], uses a frozen GNN model

Table 1: ROC-AUC (%) and standard deviation for graph classification on molecule property prediction benchmark under 50-shot scenario with various pre-training and tuning strategies. The best results for each dataset and pre-training strategy are highlighted in bold, and the runner-up is underlined.

Tuning Strategy		BBBP	Tox21	ToxCast	SIDER	ClinTox	MUV	HIV	BACE	Avg.
Infomax	FT	65.26 ±1.05	71.54 ±0.73	57.98 ±0.42	53.45 ±0.49	59.01 ±2.18	64.08 ±0.84	65.13 ±2.50	64.57 ±0.71	62.63
	GPF	66.30 ±0.94	71.26 ±0.30	58.33 ±0.27	53.65 ±0.34	63.11 ±2.35	67.19 ±0.10	64.09 ±0.66	64.32 ±0.88	63.53
	GPF-plus	66.12 ±1.27	71.54 ±0.63	58.43 ±0.27	53.76 ±1.15	65.06 ±1.56	67.20 ±0.17	64.81 ±1.62	65.88 ±1.72	64.10
	SUPT _{soft}	66.45 ±0.85	71.82 ±0.16	58.71 ±0.44	53.72 ±0.45	65.96 ±3.37	66.52 ±0.55	65.51 ±2.31	66.26 ±2.45	64.37
	SUPT _{hard}	66.14 ±0.85	71.55 ±0.37	58.65 ±0.33	53.82 ±0.49	65.90 ±3.41	66.53 ±0.35	65.59 ±2.26	66.40 ±0.70	64.32
	RELIEF	67.93 ±0.73	<u>71.58</u> ±0.13	58.78 ±0.17	<u>53.95</u> ±0.40	66.28 ±2.07	67.23 ±0.08	<u>67.00</u> ±0.55	67.95 ±0.52	65.09
AttrMasking	FT	66.48 ±0.44	72.32 ±0.19	57.35 ±0.42	54.62 ±0.58	59.71 ±4.43	61.49 ±1.04	58.37 ±1.51	65.41 ±2.09	61.97
	GPF	66.67 ±0.60	72.31 ±0.30	58.01 ±0.27	55.65 ±1.92	67.25 ±2.41	62.58 ±0.31	58.71 ±2.56	68.54 ±1.24	63.72
	GPF-plus	66.29 ±0.36	72.75 ±0.38	57.91 ±0.38	55.05 ±1.20	68.89 ±2.86	62.70 ±0.48	58.71 ±1.07	68.07 ±1.20	63.80
	SUPT _{soft}	66.28 ±0.81	72.76 ±0.41	58.28 ±0.34	54.70 ±1.03	68.58 ±4.54	62.81 ±0.25	58.95 ±1.71	66.41 ±0.49	63.60
	SUPT _{hard}	66.93 ±0.91	<u>72.75</u> ±0.41	58.18 ±0.44	55.20 ±1.26	68.36 ±3.57	<u>62.81</u> ±0.22	<u>59.02</u> ±1.61	68.92 ±0.96	64.02
	RELIEF	67.18 ±0.55	72.40 ±0.32	58.41 ±0.14	56.54 ±0.75	74.39 ±1.18	63.18 ±0.17	59.42 ±0.55	69.37 ±0.70	65.11
ContextPred	FT	<u>62.82</u> ±0.83	70.11 ±0.38	57.68 ±0.69	56.68 ±0.78	60.99 ±2.28	61.28 ±1.93	59.14 ±1.93	64.47 ±2.47	61.65
	GPF	61.65 ±0.76	70.42 ±0.29	58.51 ±0.38	56.55 ±0.46	58.80 ±2.57	64.83 ±0.32	59.68 ±2.20	68.57 ±1.19	62.38
	GPF-plus	61.25 ±0.73	70.12 ±0.42	57.64 ±0.70	56.86 ±0.52	61.43 ±3.06	64.59 ±0.28	59.15 ±2.23	68.58 ±1.42	62.45
	SUPT _{soft}	61.85 ±1.56	70.37 ±0.14	57.82 ±0.37	56.57 ±0.50	59.13 ±1.99	64.59 ±1.00	56.58 ±1.94	68.92 ±0.92	61.98
	SUPT _{hard}	62.29 ±1.41	70.40 ±0.15	58.06 ±0.39	56.34 ±0.72	59.18 ±2.07	64.57 ±0.69	59.08 ±1.47	69.40 ±1.62	62.42
	RELIEF	62.99 ±0.67	70.51 ±0.14	58.58 ±0.04	56.89 ±0.25	63.06 ±1.74	64.87 ±0.31	59.72 ±1.67	70.19 ±0.96	63.35
GCL	FT	62.13 ±1.66	61.35 ±0.88	53.96 ±0.80	52.63 ±0.71	68.73 ±4.74	51.96 ±1.93	58.67 ±1.41	49.94 ±3.80	57.42
	GPF	61.58 ±1.81	59.92 ±1.29	54.44 ±0.31	51.21 ±0.56	75.52 ±3.08	52.26 ±1.28	58.37 ±1.16	56.09 ±2.44	58.67
	GPF-plus	62.19 ±1.45	60.13 ±0.52	54.43 ±0.43	50.90 ±0.78	75.50 ±1.11	52.40 ±1.55	58.30 ±1.68	59.55 ±3.17	59.18
	SUPT _{soft}	63.96 ±0.85	60.13 ±0.52	54.57 ±0.76	51.44 ±1.24	78.03 ±2.32	51.86 ±1.48	59.30 ±2.59	57.39 ±2.64	59.59
	SUPT _{hard}	<u>64.15</u> ±0.96	60.56 ±0.20	<u>54.72</u> ±0.71	51.60 ±0.85	77.88 ±2.06	51.78 ±1.72	59.24 ±2.42	<u>59.68</u> ±1.46	<u>59.95</u>
	All in One	62.90 ±3.77	61.49 ±0.96	54.72 ±1.03	52.73 ±0.84	66.59 ±3.84	53.34 ±4.20	60.60 ±3.80	59.57 ±5.62	58.99
RELIEF	64.80 ±0.69	<u>61.45</u> ±0.35	55.03 ±0.39	52.82 ±0.59	79.75 ±1.28	53.52 ±2.17	<u>60.44</u> ±2.39	62.97 ±1.19	61.35	

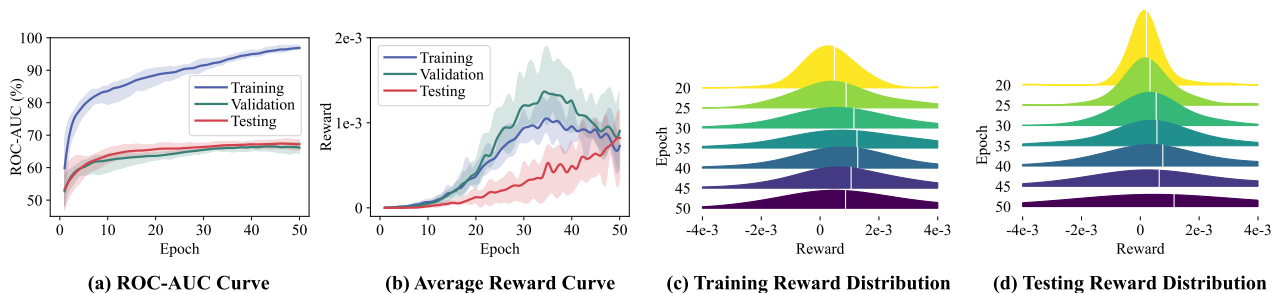


Figure 3: Tuning process of RELIEF on BACE. (a) and (b) present the ROC-AUC and average reward curves, respectively, for the training, validation, and testing sets across 5 random seeds. (c) and (d) illustrate the reward distributions for the training and testing sets as the tuning epochs progress, with white vertical lines indicating the average rewards for each distribution.

specifically pre-trained by GCL, adapting learnable graph prompts, is included as it strictly aligns with our experimental setting.

Training Scheme. Since molecular predictions are multi-label binary classifications, we use binary cross-entropy loss for the reward function and evaluate by averaging the ROC-AUC of each label. We construct few-shot scenarios with 50 samples for prompt tuning. We leverage early stopping based on validation set performance, unlike previous works that report results from the last epoch. Five rounds of experiments are conducted with different random seeds. The number of sub-policies l is set to 3, with penalty factors α_d selected from $\{1e0, 1e1, 1e3, 1e5\}$ and α_c set to 0.1. The maximum prompt scale per step z_{max} is selected from $\{0.1, 0.5, 1.0\}$. The projection head is chosen from $\{1, 2, 3\}$ -layer MLPs and trained q times per epoch, ranging from $\{1, 2, 3\}$. Detailed data splitting

Table 2: PCR, APM and overall impact (OV.) of feature prompting methods averaged on all graph classification task.

Tuning Strategy	PCR	APM (10^{-2})	OV. (10^{-2})	ROC-AUC
GPF	1.00	7.15	7.15	62.08
GPF-plus	1.00	6.69	6.69	62.38
SUPT _{soft}	1.00	6.46	6.46	62.39
SUPT _{hard}	0.65	6.10	3.97	62.68
RELIEF	0.61	6.03	3.68	63.72

and hyper-parameter settings are provided in Appendix B.3. All the experiments were conducted on an NVIDIA A800 PCIe 80GB GPU.

Performance Results. Based on the results in Table 1, our RELIEF achieves superior graph classification performance in few-shot settings, surpassing baselines in 28/32 tasks, with an average improvement of 1.64% over fine-tuning and 1.04% over the runner-up.

Table 3: The minimum proportion (%) of data required for surpassing the performance of full-shot FT. The minimum proportion are highlighted in bold. × denotes cannot surpass.

	Methods	BBBP	Tox21	SIDER	Cinltox	Bace
Infomax	GPF	×	60	60	×	55
	GPF-plus	×	60	60	65	50
	SUPT _{soft}	×	65	60	70	45
	SUPT _{hard}	×	60	55	65	50
	RELIEF	75	50	40	60	40
ContextPred	GPF	×	55	55	70	95
	GPF-plus	×	50	45	60	90
	SUPT _{soft}	×	65	50	65	85
	SUPT _{hard}	×	65	50	75	85
	RELIEF	90	50	40	55	65

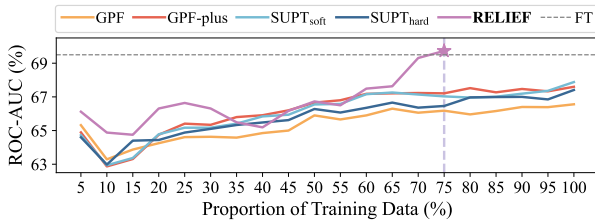


Figure 4: Performance of feature prompting methods with training data scaling up, compared to full-shot FT.

Notably, RELIEF is the only method consistently outperforming fine-tuning across all tasks. Moreover, we observe that in All in One, inserting prompt graphs with fewer nodes yields better results. This suggests that compact prompt structures may enhance prompt tuning, indirectly supporting our motivation.

We illustrate the tuning process of RELIEF on the BACE dataset pre-trained with Infomax in Figure 3. The ROC-AUC curve demonstrates a smooth and monotonically increasing trend, indicating the stability of the training process. The reward curve and distributions show reward improvement as the epochs progress, confirming the effectiveness of RELIEF’s agent in enhancing downstream task performance. Detailed tuning process analysis is in Appendix B.4.

Furthermore, we measure the impact of prompts on input graphs in terms of PCR and APM, and further multiply them to express the overall impact (OV). Results are averaged across all tasks, as outlined in Table 2. RELIEF exhibits the smallest PCR, APM and overall impact compared to baselines. Interestingly, SUPT_{hard} also prompts on specific nodes with a PCR of 0.65, as each basis prompt vector affects only the top-ranked nodes, where the top-rank ratio is a hyper-parameter, making it a rule-based node selection method. In contrast, RELIEF does not rely on priori information, such as the usage of basis vectors or a top-rank ratio, thereby offers a highly flexible prompting policy based on the actors. Notably, the flexibility of graph manipulations is crucial for prompting performance [37, 38], contributing to RELIEF’s superior results.

5.2 Data Efficiency

To evaluate the data efficiency of feature prompting methods, we incrementally add 5% of the training samples until the average ROC-AUC over five random seeds surpasses full-shot fine-tuning performance. We tune hyper-parameters after each data increment to optimize performance. We report the minimum proportion of

data required for each method to exceed fine-tuning on five datasets pre-trained with Infomax and ContextPred strategies.

Table 3 shows that RELIEF requires the least data for all tasks, while other baselines, more or less, fail to surpass full-shot fine-tuning even with the entire dataset. Figure 4 illustrates the performance trends on BBBP dataset pre-trained with Infomax, which demonstrates that RELIEF’s overall performance presents the most noticeable improvement as data scales up, whereas other methods fluctuate and ultimately fail to exceed fine-tuning.

We attribute RELIEF’s superior data efficiency to its RL-based learning paradigm, which poses two advantages. Firstly, it reduces learning difficulty by optimizing one feature prompt at a time, allowing the agent to focus on a single state-to-action mapping and avoid complex node interactions that baseline methods face when optimizing entire feature prompts at once. Secondly, the step-by-step insertion and evaluation of prompts expose the agent to various state patterns and loss values, acting as data augmentation and providing additional supervision signals in few-shot settings.

5.3 Additional Experiments

Due to space constraints, we relocate additional experiments to the Appendices. Here, we provide an overview to highlight their critical conclusions.

Node Classification (Appendix A). We extend RELIEF to node-level tasks by adding prompts to the k -hop subgraph induced by the target node [26, 37]. Experiments demonstrate RELIEF’s top-tier performance across multiple datasets compared to baselines. A case study is conducted to reveal that RELIEF can achieve its full potential when given adequately pre-trained GNN models.

Ablation Study (Appendix C). We compare RELIEF against its three variants: random discrete policy, random continuous policy, and linear probing (solely training the projection head) [19] on node and graph-level tasks. Results indicate significant performance drops when either policy is deactivated or feature prompting components are discarded.

Parameter Analysis (Appendix D). We examine the sensitivity of key hyper-parameters of RELIEF including the maximum feature prompt scale per step z_{\max} , number of sub-policies l , and penalty factors α_d and α_c . We also validate the necessity of using policy generalization techniques. The findings confirm RELIEF’s robust performance across varied hyper-parameter settings.

5.4 Why RELIEF works?

Despite of RELIEF’s superior performance in graph and node-level tasks, it is essential to explain why RELIEF, utilizing an RL framework, fulfills our motivation – achieving *powerful* downstream performance by adding *necessary* and *lightweight* prompts.

Powerful. RL demonstrates significant efficacy in solving combinatorial optimization problems [18, 28]. With a goal-oriented reward function and adequate exploration within stable state and reward dynamics, the RELIEF agent identifies an optimal prompting policy to maximize performance gains.

Necessary. The agent makes decisions based on state patterns and learned policies, displaying specific node selection preferences when faced with similar prompted features. Suboptimal node selection at any step leads to a cumulative reward decrease, which is

captured by the critic and rectified through policy updates, thereby avoiding unnecessary prompts.

Lightweight. As the case study analyzed in Appendix A.6, RELIEF tends to preserve pre-trained graph knowledge rather than overwhelm it. Larger-scale prompts cause the GNN model to generate unfamiliar representations, disrupting coordination between representations and the projection head, potentially leading to negative rewards. These punishments are applied to the actor, urging it to provide prompts that avoid excessive disturbance to the initial input through policy updates.

6 CONCLUSION

In this paper, inspired by the marginal effect of increasing prompt token length on performance improvement in LLMs, we propose RELIEF, an RL empowered graph feature prompt tuning method. RELIEF enhances the downstream performance of pre-trained GNN models by incorporating only necessary and lightweight feature prompts to original graphs. To tackle the combinatorial optimization problem, we employ an RL algorithm designed for hybrid action spaces and integrated policy generalization techniques. Extensive experiments on graph and node-level tasks demonstrate RELIEF’s effectiveness and data efficiency compared to fine-tuning and other prompt-based methods.

ACKNOWLEDGMENTS

This work is supported by National Natural Science Foundation of China No. 62202172.

REFERENCES

- [1] Tom Brown, Benjamin Mann, Nick Ryder, Melanie Subbiah, Jared D Kaplan, Prafulla Dhariwal, Arvind Neelakantan, Pranav Shyam, Girish Sastry, Amanda Askell, et al. 2020. Language models are few-shot learners. *Advances in neural information processing systems* 33 (2020), 1877–1901.
- [2] Yuwei Cao, Hao Peng, Jia Wu, Yingdong Dou, Jianxin Li, and Philip S Yu. 2021. Knowledge-preserving incremental social event detection via heterogeneous gnn. In *Proceedings of the Web Conference 2021*. 3383–3395.
- [3] Josef Dai, Xuehai Pan, Ruiyang Sun, Jiaming Ji, Xinbo Xu, Mickel Liu, Yizhou Wang, and Yaodong Yang. 2023. Safe RLHF: Safe Reinforcement Learning from Human Feedback. In *The Twelfth International Conference on Learning Representations*.
- [4] Zhou Fan, Rui Su, Weinan Zhang, and Yong Yu. 2019. Hybrid Actor-Critic Reinforcement Learning in Parameterized Action Space. In *Proceedings of the Twenty-Eighth International Joint Conference on Artificial Intelligence, IJCAI-19*. International Joint Conferences on Artificial Intelligence Organization, 2279–2285. <https://doi.org/10.24963/ijcai.2019/316>
- [5] Taoran Fang, Yunchao Zhang, Yang Yang, Chunping Wang, and Lei Chen. 2024. Universal prompt tuning for graph neural networks. *Advances in Neural Information Processing Systems* 36 (2024).
- [6] Qingqing Ge, Zeyuan Zhao, Yiding Liu, Anfeng Cheng, Xiang Li, Shuaiqiang Wang, and Dawei Yin. 2024. PSP: Pre-Training and Structure Prompt Tuning for Graph Neural Networks. arXiv:2310.17394 [cs.LG] <https://arxiv.org/abs/2310.17394>
- [7] Dibya Ghosh, Jad Rahme, Aviral Kumar, Amy Zhang, Ryan P Adams, and Sergey Levine. 2021. Why generalization in rl is difficult: Epistemic pomdps and implicit partial observability. *Advances in neural information processing systems* 34 (2021), 25502–25515.
- [8] Chenghua Gong, Xiang Li, Jianxiang Yu, Cheng Yao, Jiaqi Tan, and Chengcheng Yu. 2024. Self-Pro: A Self-Prompt and Tuning Framework for Graph Neural Networks. arXiv:2310.10362 [cs.LG] <https://arxiv.org/abs/2310.10362>
- [9] Xueting Han, Zhenhuan Huang, Bang An, and Jing Bai. 2021. Adaptive transfer learning on graph neural networks. In *Proceedings of the 27th ACM SIGKDD Conference on Knowledge Discovery & Data Mining*. 565–574.
- [10] Shengding Hu, Zheng Xiong, Meng Qu, Xingdi Yuan, Marc-Alexandre Côté, Zhiyuan Liu, and Jian Tang. 2020. Graph policy network for transferable active learning on graphs. *Advances in Neural Information Processing Systems* 33 (2020), 10174–10185.
- [11] Weihua Hu, Bowen Liu, Joseph Gomes, Marinka Zitnik, Percy Liang, Vijay Pande, and Jure Leskovec. 2019. Strategies for pre-training graph neural networks. *arXiv preprint arXiv:1905.12265* (2019).
- [12] Shengyi Huang, Rousslan Fernand Julien Dossa, Antonin Raffin, Anssi Kanervisto, and Weixun Wang. 2022. The 37 Implementation Details of Proximal Policy Optimization. In *ICLR Blog Track*. <https://iclr-blog-track.github.io/2022/03/25/ppo-implementation-details/> <https://iclr-blog-track.github.io/2022/03/25/ppo-implementation-details/>.
- [13] Menglin Jia, Luming Tang, Bor-Chun Chen, Claire Cardie, Serge Belongie, Bharath Hariharan, and Ser-Nam Lim. 2022. Visual prompt tuning. In *European Conference on Computer Vision*. Springer, 709–727.
- [14] Minqi Jiang, Edward Grefenstette, and Tim Rocktäschel. 2021. Prioritized Level Replay. In *Proceedings of the 38th International Conference on Machine Learning, ICML 2021, 18–24 July 2021, Virtual Event (Proceedings of Machine Learning Research, Vol. 139)*, Marina Meila and Tong Zhang (Eds.). PMLR, 4940–4950. <http://proceedings.mlr.press/v139/jiang21b.html>
- [15] Yangqin Jiang, Chao Huang, and Lianghao Huang. 2023. Adaptive graph contrastive learning for recommendation. In *Proceedings of the 29th ACM SIGKDD conference on knowledge discovery and data mining*. 4252–4261.
- [16] Thomas N. Kipf and Max Welling. 2017. Semi-Supervised Classification with Graph Convolutional Networks. In *5th International Conference on Learning Representations, ICLR 2017, Toulon, France, April 24–26, 2017, Conference Track Proceedings*. OpenReview.net. <https://openreview.net/forum?id=SJU4ayYgl>
- [17] Alexander Kirillov, Eric Mintun, Nikhila Ravi, Hanzi Mao, Chloe Rolland, Laura Gustafson, Tete Xiao, Spencer Whitehead, Alexander C Berg, Wan-Yen Lo, et al. 2023. Segment anything. In *Proceedings of the IEEE/CVF International Conference on Computer Vision*. 4015–4026.
- [18] Lecheng Kong, Jiarui Feng, Hao Liu, Dacheng Tao, Yixin Chen, and Muhan Zhang. 2024. MAG-GNN: Reinforcement Learning Boosted Graph Neural Network. *Advances in Neural Information Processing Systems* 36 (2024).
- [19] Ananya Kumar, Aditi Raghunathan, Robbie Matthew Jones, Tengyu Ma, and Percy Liang. 2022. Fine-Tuning can Distort Pretrained Features and Underperform Out-of-Distribution. In *The Tenth International Conference on Learning Representations, ICLR 2022, Virtual Event, April 25–29, 2022*. OpenReview.net. <https://openreview.net/forum?id=UYneFzXSJWh>
- [20] Junhyun Lee, Woosong Yang, and Jaewoo Kang. 2024. Subgraph-level Universal Prompt Tuning. *arXiv preprint arXiv:2402.10380* (2024).
- [21] Brian Lester, Rami Al-Rfou, and Noah Constant. 2021. The Power of Scale for Parameter-Efficient Prompt Tuning. In *Proceedings of the 2021 Conference on Empirical Methods in Natural Language Processing, EMNLP 2021, Virtual Event / Punta Cana, Dominican Republic, 7–11 November, 2021, Marie-Francine Moens, Xuanjing Huang, Lucia Specia, and Scott Wen-tau Yih (Eds.)*. Association for Computational Linguistics, 3045–3059. <https://doi.org/10.18653/V1/2021.EMNLP-MAIN.243>
- [22] Xiang Lisa Li and Percy Liang. 2021. Prefix-Tuning: Optimizing Continuous Prompts for Generation. In *Proceedings of the 59th Annual Meeting of the Association for Computational Linguistics and the 11th International Joint Conference on Natural Language Processing, ACL/IJCNLP 2021, (Volume 1: Long Papers), Virtual Event, August 1–6, 2021*, Chengqing Zong, Fei Xia, Wenjie Li, and Roberto Navigli (Eds.). Association for Computational Linguistics, 4582–4597. <https://doi.org/10.18653/V1/2021.ACL-IJCNLP.353>
- [23] Ke Liang, Yue Liu, Sihang Zhou, Wenxuan Tu, Yi Wen, Xihong Yang, Xiangjun Dong, and Xinwang Liu. 2023. Knowledge graph contrastive learning based on relation-symmetrical structure. *IEEE Transactions on Knowledge and Data Engineering* (2023).
- [24] Huihui Liu, Yiding Yang, and Xinchao Wang. 2021. Overcoming catastrophic forgetting in graph neural networks. In *Proceedings of the AAAI conference on artificial intelligence*, Vol. 35. 8653–8661.
- [25] Pengfei Liu, Weizhe Yuan, Jinlan Fu, Zhengbao Jiang, Hiroaki Hayashi, and Graham Neubig. 2023. Pre-train, Prompt, and Predict: A Systematic Survey of Prompting Methods in Natural Language Processing. *ACM Comput. Surv.* 55, 9, Article 195 (jan 2023), 35 pages. <https://doi.org/10.1145/3560815>
- [26] Zemin Liu, Xingtong Yu, Yuan Fang, and Xinming Zhang. 2023. Graphprompt: Unifying pre-training and downstream tasks for graph neural networks. In *Proceedings of the ACM Web Conference 2023*. 417–428.
- [27] Warwick Masson, Praveesh Ranchor, and George Konidaris. 2016. Reinforcement learning with parameterized actions. In *Proceedings of the AAAI conference on artificial intelligence*, Vol. 30.
- [28] Nina Mazyavkina, Sergey Sviridov, Sergei Ivanov, and Evgeny Burnaev. 2021. Reinforcement learning for combinatorial optimization: A survey. *Computers & Operations Research* 134 (2021), 105400.
- [29] Long Ouyang, Jeffrey Wu, Xu Jiang, Diogo Almeida, Carroll Wainwright, Pamela Mishkin, Chong Zhang, Sandhini Agarwal, Katarina Slama, Alex Ray, et al. 2022. Training language models to follow instructions with human feedback. *Advances in neural information processing systems* 35 (2022), 27730–27744.
- [30] Roberta Raileanu and Rob Fergus. 2021. Decoupling value and policy for generalization in reinforcement learning. In *International Conference on Machine Learning*. PMLR, 8787–8798.

- [31] Bharath Ramsundar, Peter Eastman, Pat Walters, and Vijay Pande. 2019. *Deep learning for the life sciences: applying deep learning to genomics, microscopy, drug discovery, and more*. " O'Reilly Media, Inc".
- [32] John Schulman, Philipp Moritz, Sergey Levine, Michael Jordan, and Pieter Abbeel. 2015. High-dimensional continuous control using generalized advantage estimation. *arXiv preprint arXiv:1506.02438* (2015).
- [33] John Schulman, Filip Wolski, Prafulla Dhariwal, Alec Radford, and Oleg Klimov. 2017. Proximal policy optimization algorithms. *arXiv preprint arXiv:1707.06347* (2017).
- [34] Oleksandr Shchur, Maximilian Mumme, Aleksandar Bojchevski, and Stephan Günnemann. 2018. Pitfalls of graph neural network evaluation. *arXiv preprint arXiv:1811.05868* (2018).
- [35] Mingchen Sun, Kaixiong Zhou, Xin He, Ying Wang, and Xin Wang. 2022. Gppt: Graph pre-training and prompt tuning to generalize graph neural networks. In *Proceedings of the 28th ACM SIGKDD Conference on Knowledge Discovery and Data Mining*. 1717–1727.
- [36] Qingyun Sun, Jianxin Li, Hao Peng, Jia Wu, Yuanxing Ning, Philip S Yu, and Lifang He. 2021. Sugar: Subgraph neural network with reinforcement pooling and self-supervised mutual information mechanism. In *Proceedings of the Web Conference 2021*. 2081–2091.
- [37] Xiangguo Sun, Hong Cheng, Jia Li, Bo Liu, and Jihong Guan. 2023. All in one: Multi-task prompting for graph neural networks. In *Proceedings of the 29th ACM SIGKDD Conference on Knowledge Discovery and Data Mining*. 2120–2131.
- [38] Xiangguo Sun, Jiawen Zhang, Xixi Wu, Hong Cheng, Yun Xiong, and Jia Li. 2023. Graph prompt learning: A comprehensive survey and beyond. *arXiv preprint arXiv:2311.16534* (2023).
- [39] Richard S Sutton and Andrew G Barto. 2018. *Reinforcement learning: An introduction*. MIT press.
- [40] Petar Veličković, William Fedus, William L Hamilton, Pietro Liò, Yoshua Bengio, and R Devon Hjelm. 2018. Deep graph infomax. *arXiv preprint arXiv:1809.10341* (2018).
- [41] Kaixin Wang, Bingyi Kang, Jie Shao, and Jiashi Feng. 2020. Improving generalization in reinforcement learning with mixture regularization. *Advances in Neural Information Processing Systems* 33 (2020), 7968–7978.
- [42] Kaixin Wang, Cheng Long, Da Yan, Jie Zhang, and HV Jagadish. 2023. Reinforcement learning enhanced weighted sampling for accurate subgraph counting on fully dynamic graph streams. In *2023 IEEE 39th International Conference on Data Engineering (ICDE)*. IEEE, 1084–1097.
- [43] Lirong Wu, Haitao Lin, Cheng Tan, Zhangyang Gao, and Stan Z Li. 2021. Self-supervised learning on graphs: Contrastive, generative, or predictive. *IEEE Transactions on Knowledge and Data Engineering* 35, 4 (2021), 4216–4235.
- [44] Zhenqin Wu, Bharath Ramsundar, Evan N Feinberg, Joseph Gomes, Caleb Geniesse, Aneesh S Pappu, Karl Leswing, and Vijay Pande. 2018. MoleculeNet: a benchmark for molecular machine learning. *Chemical science* 9, 2 (2018), 513–530.
- [45] Yaochen Xie, Zhao Xu, Jingtun Zhang, Zhengyang Wang, and Shuiwang Ji. 2022. Self-supervised learning of graph neural networks: A unified review. *IEEE transactions on pattern analysis and machine intelligence* 45, 2 (2022), 2412–2429.
- [46] Jiechao Xiong, Qing Wang, Zhuoran Yang, Peng Sun, Lei Han, Yang Zheng, Haobo Fu, Tong Zhang, Ji Liu, and Han Liu. 2018. Parametrized deep q-networks learning: Reinforcement learning with discrete-continuous hybrid action space. *arXiv preprint arXiv:1810.06394* (2018).
- [47] Keyulu Xu, Weihua Hu, Jure Leskovec, and Stefanie Jegelka. 2018. How powerful are graph neural networks? *arXiv preprint arXiv:1810.00826* (2018).
- [48] Hantao Yao, Rui Zhang, and Changsheng Xu. 2023. Visual-language prompt tuning with knowledge-guided context optimization. In *Proceedings of the IEEE/CVF Conference on Computer Vision and Pattern Recognition*. 6757–6767.
- [49] Gilad Yehudai, Ethan Fetaya, Eli Meir, Gal Chechik, and Haggai Maron. 2021. From local structures to size generalization in graph neural networks. In *International Conference on Machine Learning*. PMLR, 11975–11986.
- [50] Yuning You, Tianlong Chen, Yongduo Sui, Ting Chen, Zhangyang Wang, and Yang Shen. 2020. Graph Contrastive Learning with Augmentations. *Advances in Neural Information Processing Systems* 33 (2020), 5812–5823.
- [51] Chengcheng Yu, Jiapeng Zhu, and Xiang Li. 2024. GraphCBAL: Class-Balanced Active Learning for Graph Neural Networks via Reinforcement Learning. In *Proceedings of the 33rd ACM International Conference on Information and Knowledge Management (Boise, ID, USA) (CIKM '24)*. Association for Computing Machinery, New York, NY, USA, 3022–3031. <https://doi.org/10.1145/3627673.3679624>
- [52] Qi Zhu, Bing Li, Fei Mi, Xiaoyan Zhu, and Minlie Huang. 2022. Continual Prompt Tuning for Dialog State Tracking. In *Proceedings of the 60th Annual Meeting of the Association for Computational Linguistics (Volume 1: Long Papers), ACL 2022, Dublin, Ireland, May 22–27, 2022*, Smaranda Muresan, Preslav Nakov, and Aline Villavicencio (Eds.). Association for Computational Linguistics, 1124–1137. <https://doi.org/10.18653/V1/2022.ACL-LONG.80>
- [53] Yun Zhu, Jianhao Guo, and Siliang Tang. 2023. Sgl-pt: A strong graph learner with graph prompt tuning. *arXiv preprint arXiv:2302.12449* (2023).

A FEW-SHOT NODE CLASSIFICATION

A.1 Extend to Node-Level Tasks

Given that feature prompting methods are originally designed to address graph-level tasks [5], adapting them to node-level tasks requires careful consideration.

Fortunately, prior research has successfully unified various levels of tasks as subgraph-level tasks [26, 37]. This unification is achieved by generating induced graphs for nodes or edges, which enables feature prompting methods to operate on k -hop subgraphs. These subgraphs act as proxies for the target nodes or edges during prompt tuning and downstream tasks evaluation. Here, we examine the capability of RELIEF on node classification tasks, alongside other existing feature prompting approaches.

A.2 Details of Datasets

We adopt Cora, Citeseer and Pubmed [16] and Amazon-Co-Buy (Computer and Photo) [34] for node classification. Cora, Citeseer, and Pubmed are citation networks, where each node represents a publication with a sparse bag-of-words feature vector, and edges signify citation links. Computer and Photo are segments of the Amazon co-purchase graph, with nodes representing products, edges indicating frequent co-purchases, node features encoded as bag-of-words from product reviews, and class labels derived from product categories. The statistics of these dataset are summarized in Table 4.

A.3 Details of Pre-training Strategies

To complement the node and graph-level pre-training strategies used in graph classification experiments, we focus on edge-level pre-training strategies to demonstrate the generality of RELIEF. Therefore, we include all previously mentioned feature prompting methods and additionally involve GPPT [35] and GraphPrompt [26] as baselines, which are tailored to GNN models pre-trained at edge-level and capable of transferring to node classification.

Formally, GPPT uses masked edge prediction (MaskedEdge) as pretext task, which is optimized by a binary cross-entropy loss $\mathcal{L}(\cdot)$ formulated as:

$$\min_{\theta} \sum_{v_i, v_j} \mathcal{L}(f_{\theta}(v_i)^{\top} f_{\theta}(v_j), \mathbf{A}_{ij})$$

where \mathbf{A}_{ij} represents if node v_i and v_j are connected given graph \mathcal{G} with the adjacency matrix \mathbf{A} . Moreover, GraphPrompt employs contrastive learning using positive and negative node pairs determined based on edge connectivity (ContraEdge). The pre-training loss is defined as follows:

$$\min_{\theta} -\frac{1}{|\mathcal{V}|} \sum_{v \in \mathcal{V}} \frac{1}{|\mathcal{V}^+|} \sum_{v^+ \in \mathcal{N}(v)} \log \frac{\exp(h_v^{\top} h_{v^+} / \tau)}{\exp(h_v^{\top} h_{v^+} / \tau) + \sum_{v^- \in \mathcal{V}^-} \exp(h_v^{\top} h_{v^-} / \tau)}$$

where h_v , h_{v^+} and h_{v^-} are representations of node v , v^+ and v^- produced by $f_{\theta}(\mathcal{G})$. \mathcal{V}^+ is the positive node set containing the neighbors of node v , while \mathcal{V}^- is the negative node set constructed by random sampling. τ is the temperature hyper-parameter.

Table 4: Statistics of the datasets used in our node classification experiments.

Dataset	# Nodes	# Edges	# Features	# Classes
Cora	2708	5429	1433	7
CiteSeer	3327	9104	3703	6
PubMed	19717	88648	500	3
Computers	13752	491722	767	10
Photo	7650	238162	745	8

A.4 Experimental Settings

Data splitting and preprocessing. We construct 10-shot node classification experiments by randomly sampling 10 nodes per class, with additional 500 nodes each for validation and testing. Considering the average degree of different datasets, we set varying k for generating k -hop subgraphs, specifically 4, 3, 2, 2 for Cora, Citeseer, Pubmed, Computers and Photo, respectively, to ensure an appropriate number of nodes for induced subgraphs.

Implementation. We employ a 2-layer GIN [47] as the fundamental GNN model, which is widely utilized in previous works [16, 34, 35], with a hidden dimension of 128. While more advanced subgraph GNN techniques might yield better performance, as noted in [5], we opt to use the basic GIN for processing prompted subgraphs to ensure a fair comparison with GPPT and GraphPrompt, as these two methods do not incorporate subgraph-related designs. To achieve more compact node representations, we use Singular Value Decomposition (SVD) to reduce the initial features of each dataset to 100 dimensions. Cross-entropy loss is used as the reward function. The policy network and the projection head are independently updated using two Adam optimizers. Other hyper-parameters are listed in Table 6. The RL hyper-parameter settings are partly referenced from [14], aligning with its established terminology.

A.5 Performance Results

To evaluate the prompt tuning methods, we conducted five rounds of experiments with different random seeds, assessing performance using accuracy and macro F1-score. As illustrated in Table 5, RELIEF consistently achieves top-tier performance across majority of tasks, frequently ranking either first or as the runner-up, underscoring its applicability and effectiveness. On average, RELIEF outperforms fine-tuning by 2.05% and 1.43% on accuracy and macro f1-score, respectively. Additionally, RELIEF surpasses the second-best method, GPF-plus, by 0.89% in accuracy.

In contrast, GPPT and GraphPrompt exhibit inferior performance in most tasks. A plausible explanation is that their prediction results rely on class prototypes, which are challenging to accurately construct in few-shot scenarios with limited labeled data.

A.6 Case Study

One notable observation, as demonstrated in Table 5, is that RELIEF’s performance lags behind its usual advantage in other tasks on the Computers dataset with GIN pre-trained by MaskedEdge. We thus conduct a case study to investigate the underlying causes.

Despite employing various widely-used training techniques – such as dynamically reducing the learning rate, altering batch sizes, applying weight decay in the Adam optimizer, and adjusting the

Table 5: Accuracy (%) and Macro F1-score (%) with respective standard deviation for node classification under 10-shot scenario with various two edge-level pre-training and various tuning strategies. The best results for each dataset and pre-training strategy are highlighted in bold, and the runner-up is underlined.

Tuning Strategy	Cora		CiteSeer		PubMed		Computers		Photos		
	Accuracy	Macro F1	Accuracy	Macro F1	Accuracy	Macro F1	Accuracy	Macro F1	Accuracy	Macro F1	
MaskedEdge	FT	54.40 ±1.44	53.27 ±1.45	61.28 ±0.93	56.60 ±0.92	71.40 ±1.61	67.11 ±1.51	80.52 ±1.18	76.35 ±1.57	83.40 ±3.00	81.31 ±2.88
	GPF	55.04 ±1.82	54.20 ±2.03	60.48 ±1.11	55.57 ±0.97	64.96 ±6.77	60.63 ±5.17	73.32 ±2.56	68.53 ±2.21	83.08 ±0.68	80.60 ±1.04
	GPF-plus	56.36 ±1.46	55.84 ±1.33	<u>61.36</u> ±0.70	56.50 ±0.44	<u>72.32</u> ±4.17	<u>67.52</u> ±3.51	80.56 ±1.97	76.69 ±1.87	85.08 ±1.22	82.26 ±0.94
	SUPT _{soft}	55.24 ±1.01	54.69 ±1.18	59.60 ±1.97	54.88 ±1.45	62.40 ±7.67	58.76 ±6.17	77.28 ±4.18	72.63 ±4.86	84.52 ±1.55	82.22 ±1.36
	SUPT _{hard}	56.96 ±1.28	55.86 ±1.28	61.28 ±1.84	<u>56.81</u> ±1.45	71.64 ±5.98	65.20 ±5.70	77.96 ±1.61	73.60 ±1.72	85.24 ±0.81	<u>82.92</u> ±0.56
	GPPT	45.76 ±0.34	46.05 ±0.30	57.00 ±0.55	51.03 ±0.68	71.36 ±0.70	64.53 ±0.84	75.80 ±0.42	69.97 ±0.57	82.48 ±0.74	80.65 ±0.71
	RELIEF	<u>56.76</u> ±0.23	55.94 ±0.25	65.16 ±1.21	58.55 ±1.12	72.36 ±1.05	<u>66.71</u> ±1.10	77.68 ±0.93	72.53 ±1.26	<u>85.16</u> ±0.89	84.07 ±0.69
ContraEdge	FT	60.60 ±1.89	59.82 ±2.01	60.88 ±2.79	<u>56.90</u> ±2.20	72.20 ±1.02	67.44 ±0.81	80.64 ±1.23	76.02 ±1.75	82.24 ±1.92	79.71 ±1.79
	GPF	59.12 ±1.95	58.70 ±1.92	63.24 ±3.09	55.00 ±2.54	71.24 ±1.98	66.35 ±2.84	80.68 ±1.48	76.29 ±1.60	83.64 ±1.30	81.33 ±1.27
	GPF-plus	60.60 ±1.08	<u>60.63</u> ±0.87	62.44 ±1.86	56.81 ±0.55	<u>73.64</u> ±3.73	<u>69.95</u> ±3.67	80.68 ±0.65	<u>76.93</u> ±0.92	86.20 ±1.15	83.57 ±1.19
	SUPT _{soft}	60.28 ±1.32	60.05 ±1.08	63.16 ±2.35	55.95 ±1.69	73.52 ±3.81	69.70 ±3.31	80.84 ±0.85	75.30 ±0.81	85.36 ±1.75	82.47 ±1.94
	SUPT _{hard}	58.92 ±0.86	58.75 ±0.82	<u>64.32</u> ±2.38	55.96 ±2.20	73.56 ±1.97	69.48 ±2.18	80.52 ±0.95	76.69 ±0.87	86.28 ±0.55	83.92 ±0.34
	GPrompt	57.20 ±2.13	53.98 ±2.82	59.52 ±0.65	55.46 ±0.70	70.00 ±0.62	66.17 ±0.51	67.44 ±0.80	64.81 ±1.42	<u>74.08</u> ±2.55	71.26 ±2.66
	RELIEF	61.20 ±1.20	60.89 ±0.91	66.28 ±0.27	58.01 ±0.32	74.96 ±1.72	70.22 ±1.70	82.04 ±0.83	78.03 ±0.77	86.48 ±0.90	<u>83.88</u> ±0.62

Table 6: Hyper-parameter settings for graph and node level tasks.

Hyper-parameter	graph-level	node-level
<i>General Hyper-parameters</i>		
# Training epochs	{50, 100}	{50, 100, 300}
Graph loader batch size	{8, 16, 32, 64}	
# GIN layers	5	2
GIN hidden dimension	300	128
Dropout ratio	0.5	
Actors learning rate (lr)	5e-4	
# Sub-policies l	3	
Discrete actors penalty α_d	{1e0, 1e1, 1e3, 1e5}	
Continuous actors penalty α_c	0.1	
Critic lr	5e-4	
Maximum prompt scale z_{\max}	{0.1, 0.5, 1.0}	{0.05, 0.1, 0.5}
Policy network weight decay	1e-5	
Policy network lr linear decay	{True, False}	
Projection head lr	{5e-4, 1e-3, 1.5e-3}	
# Projection head layers	{1, 2, 3}	
# Projection head updates q	{1, 2, 3}	
Projection head weight decay	0	5e-4
Projection head lr linear decay	{True, False}	
<i>RL Hyper-parameters</i>		
Discount factor γ	0.99	
GAE λ	0.95	
# PPO epochs	10	
PPO mini-batch size	{32, 64, 128, 256, 512}	
PPO clip range	0.2	
Return normalization	True	
Entropy bonus coefficient β	0.01	
Critic loss coefficient	0.5	

dropout ratio – the self-supervised pre-training loss of the GIN model in this case still fails to decrease steadily. This indicates inadequate pre-training of the GNN model.

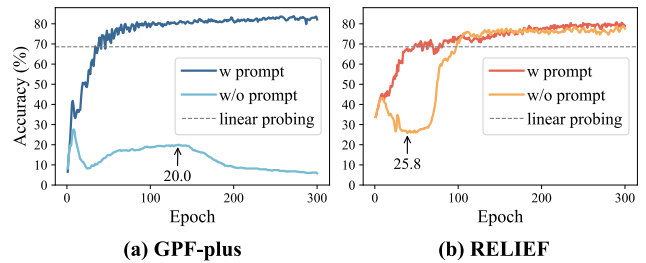


Figure 5: The testing accuracy of RELIEF and GPF-plus with and without feature prompts.

To investigate the discrepancy between GPF-plus (which performs best under this scenario) and RELIEF, we examine testing accuracy curves with and without incorporating prompts. As depicted in Figure 5, for GPF-plus, the testing accuracy without prompts rises at early epochs, reaching a maximum of 20.0, but then almost monotonically decreases to around 7.0, worse than random guessing in the ten-class classification task on the Computers dataset. Conversely, for RELIEF, although there is a downward trend in the first 50 epochs, with a minimum accuracy of 25.8, the accuracy then rapidly increases to about 75.1 and gradually converges.

We attribute the discrepancy in testing accuracy to different extents of disturbance caused by feature prompts, supported by two aspects. Firstly, we compare the APM (Average Prompt Magnitude) of GPF-plus and RELIEF, which are 0.194 and 0.053, respectively, against the original feature scale of 0.502, computed by the mean of L1-norm of each initial node feature averaged on dimension. Additionally, GPF-plus prompts on all nodes while RELIEF has a PCR (Prompt Coverage Ratio) of 0.61. Secondly, we apply linear probing [19] to this case by solely adjusting the projection head, which is widely used in NLP domain to evaluate the expressiveness of the pre-trained model. The final testing accuracy of linear probing is 68.6, as indicated by a horizontal dotted gray line in Figure 5. When discarding prompts, GPF-plus's accuracy plummets from 68.6 to 7.0, implying it overrides the initial features with overwhelming prompts, resulting in the pre-trained representations (obtained by directly feeding the original node features into the pre-trained

GNN) becoming ineffective. In contrast, RELIEF maintains pre-trained knowledge and further generalizes it, leading to an accuracy increase from 68.6 to 77.6.

This raises the question: *Why does GPF-plus excel while RELIEF struggles to show its effectiveness?* With an inadequately pre-trained GNN model, which neither provides differentiated representations based on initial features nor adjusts itself during prompt tuning, GPF-plus relies on larger feature prompts to create differences in the input space. As a result, it generates discriminative representations better aligned with training labels via the collaboration between prompts and the projection head.

However, this scenario poses challenges for our RL-based RELIEF. As discussed in Section 3.2, the essence of RL is to map states to actions or to state-value functions. Actors are guided by state-values to explore and update, with state-values computed based on rewards. Thus, capturing the relationships between states and rewards is crucial for a powerful agent. In our scenario, states are constructed on node representations, and rewards are derived from the loss function. However, with the GNN model’s insufficient capacity, it may provide similar representations for samples with different labels and distinct representations for samples of the same class. Consequently, a trajectory (composed of transitions sampled on a single graph during exploration) effective on one graph may fail on another graph with similar representations but different labels. This leads to contradictory transitions, distracting the critic from accurately estimating state-value functions, thereby increasing the difficulty of obtaining the optimal policy.

In summary, GPF-plus tends to overshadow the original input to build a new mapping when faced with an inadequately pre-trained GNN model, while RELIEF performs well by interacting in an environment with stable reward dynamics provided by adequately pre-trained models. Therefore, RELIEF and GPF-plus can excel in complementary settings, where well-pre-trained models are more likely to be encountered and are preferable.

B MORE INFORMATION ON GRAPH CLASSIFICATION

For datasets and pre-training strategies used in graph classification, we adhere to the training procedures established by pioneering researchers [11], with pre-trained GIN models available on their GitHub repository ¹.

B.1 Details of Datasets

Chemical datasets [11] are used to pre-train GNN models, consisting of both unlabeled and labeled molecules to facilitate comprehensive model training. Specifically, 2 million unlabeled molecules from the ZINC15 database are utilized for node-level self-supervised pre-training. For graph-level multi-task supervised pre-training, a preprocessed subset of the ChEMBL database including 456k labeled molecules is used, offering a diverse chemical space that enhances the model’s ability to generalize across various biochemical tasks.

For downstream graph classification tasks, 8 binary classification datasets for molecular property prediction about biophysics and physiology [44] are employed. The statistics of these downstream datasets are summarized in Table 7.

¹https://github.com/snap-stanford/pretrain-gnns/tree/master/chem/model_gin

Table 7: Statistics of the downstream datasets used in our graph classification experiments.

Dataset	# Molecules	# Tasks	Dataset	# Molecules	# Tasks
BBBP	2039	1	ClinTox	1478	2
Tox21	7831	12	MUV	93087	17
ToxCast	8575	617	HIV	41127	1
SIDER	1427	27	BACE	1513	1

B.2 Details of Pre-training Strategies

Four pre-training strategies are used to assess the universal applicability of prompting approaches.

Deep Graph Infomax (Infomax) [40] aims to derive expressive representations for graphs or nodes by maximizing the mutual information between the overall graph-level representations and the substructure-level representations at various granularities.

Attribute Masking (AttrMasking) [11] involves obscuring certain node or edge attributes. GNN models are then tasked with predicting these masked attributes based on the surrounding structural information.

Context Prediction (ContextPred) [11] uses subgraphs to predict their surrounding graph structures, which is designed to map nodes that appear in similar structural contexts to nearby embeddings, thereby capturing the context in which nodes are found.

Graph Contrastive Learning (GCL) [50] focuses on embedding augmented versions of the same anchor closely together (positive samples) while pushing the embeddings of different samples (negatives) apart.

The GNN models are first pre-trained using one of the above self-supervised methods and follow by the graph-level multi-task supervised pre-training.

B.3 Experimental Settings

We divide each dataset into training, validation, and testing sets with ratios of 80%, 10%, and 10%, respectively. Molecules are divided based on their scaffolds, i.e., molecular graph substructures [31], and the clusters are recombined by prioritizing the most frequently occurring scaffolds in the training set. This produces validation and testing sets containing structurally different molecules [11], allowing us to evaluate the model’s out-of-distribution generalization.

To create 50-shot scenarios, we randomly sampled 50 graphs from the training set, contrasting with the original 1.1k to 74k training samples. This procedure introduced randomness, differing from previous works [5, 20] that selected training data in descending order of scaffold occurrence. Given the limited budget of only 50 samples, the prior method resulted in training data with very few scaffold types, exacerbating overfitting. Consequently, the average ROC-AUC of fine-tuning across tasks under the 50-shot setting reported in previous works [5, 20] was $55.40 \pm 2.13\%$, slightly above a random guess for binary classification tasks, thus potentially reducing the performance discrepancy between each prompting method. In contrast, our randomness brings about a dataset with more molecular diversity and also prevents scaffold overlap between training, validation and test sets. As a result, the average ROC-AUC of fine-tuning under our data splitting method is 60.92% with a smaller standard deviation of 1.46%.

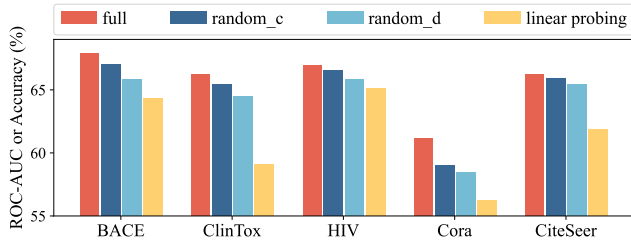


Figure 6: Effectiveness of discrete and continuous policies.

We employ a 5-layer GIN with hidden dimensions of 300 as the base model. The policy network and the projection head are independently updated using two Adam optimizers. We assess downstream task performance using the validation early stopping protocol, reporting the test ROC-AUC at the best validation epoch. Additionally, considering that 50-shot learning may be insufficient for some datasets to ensure stable performance at the onset of training, we determine the best validation epoch after 20 epochs. The complete hyper-parameters for graph classification are detailed listed in Table 6.

B.4 Tuning Process Analysis

We analyze RELIEF’s tuning process on BACE using a GIN pre-trained with Infomax. In Figure 3, “Reward” denotes the cumulative reward for each graph, and “Average Reward” is the mean “Reward” over a graph set.

Figure 3(a) shows that the ROC-AUC scores for the training, validation, and testing sets consistently increase during tuning, with validation performance converging around 50 epochs. Figure 3(b) illustrates the average reward induced by RELIEF’s prompting policy. Since scaffold splitting results in similar data distributions for the training and validation sets, their reward curves are also similar, increasing during the first 35 epochs and then gently decreasing. This decrease is due to the penalty aimed at improving policy generalization. As sub-policies diverge and produce distinct actions, the penalty – which measures the divergence between each sub-policy and the joint policy – increases. This prevents the joint policy from adhering to local contexts, thus enhancing generalization, though it leads to a rewards drop. Consequently, the testing set’s average reward rises steadily, indicating good generalization.

Figure 3(c) and (d) depict the reward distributions for the training and testing sets from 20 to 50 epochs, using the same random seed. The white vertical lines indicate average rewards at different epochs, showing a similar trend to Figure 3(b). In the early stages, such as at 20 epochs, rewards hover near 0. This resembles attaching random feature prompts to the original feature space, akin to data augmentation, which contributes to a more robust projection head. As tuning progresses, the policy network learns to map states to actions more discriminatively, resulting in broader reward distributions with an almost monotonically increasing mean for the testing set.

C ABLATION STUDY

Considering the core of RELIEF lies in its two actors for incorporating feature prompts, we deactivated either one to create two

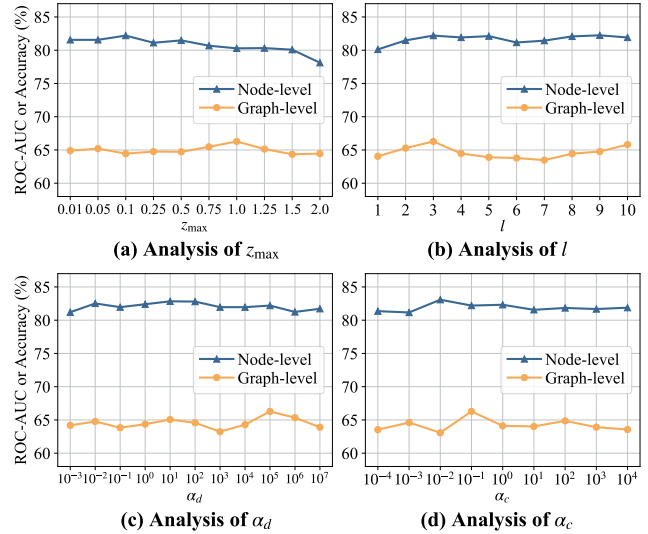


Figure 7: Parameter sensitivity analysis.

variants. Specifically, “random_d” replaces the discrete policy by randomly sampling a valid node to prompt at each step, while “random_c” replaces the continuous policy with a real-valued vector sampled from a random Gaussian distribution. Additionally, we include “linear probing” [19], which discards the prompting components and adjusts only the projection head.

Figure 6 shows the comparisons of RELIEF with its variants on three graph-level and two node-level tasks. We find that deactivating either actor results in an obvious performance drop due to the disruption of their coordination. Particularly, the discrete actor plays a crucial role in RELIEF. Intuitively, a random prompt context assigned to a target node can be rectified by prompting on the node again in later steps, given the premise of a powerful discrete actor for locating this node. However, with a random node selection policy, a suboptimal feature prompt is difficult to mitigate by prompting on arbitrary nodes, and is further exacerbated by the message-passing mechanism, which spreads chaotic prompts throughout the graph. In addition, “linear probing”, which only trains the projection head, exhibits significantly inferior performance, clearly demonstrating the contribution of the inserted feature prompts.

D PARAMETER ANALYSIS

We analyze the critical hyper-parameters in RELIEF, including the maximum feature prompt scale per step z_{max} , the number of sub-policies l , and the two penalty factors α_d and α_c related to policy generalization. Figure 7 illustrates the ROC-AUC on ClinTox and accuracy on Computers, representing graph and node-level tasks, with each hyper-parameter varied over its legal range of values. The observations are as follows:

From Figure 7, we have the following observations. RELIEF performs consistently well across a broad range of hyper-parameter values, demonstrating its robustness. Specifically, when z_{max} is too large, the excessive magnitude of prompts introduces unnecessary disturbance, leading to performance degradation. Conversely, setting z_{max} too small weakens the impact of feature prompting,

making it more similar to linear probing. By setting l to 1, which discards the policy generalization technique, results in significant performance decline. While increasing l may improve performance, it also requires maintaining more pairs of actors, leading to computational overhead. For α_d and α_c , excessively large values may result in overly punishment, making the policies too conservative and hindering performance improvements.

E INTRODUCTION TO PPO AND H-PPO

Under our feature prompting scenario, an MDP is denoted as a tuple $\langle \mathcal{S}, \mathcal{A}_d, \mathcal{A}_c, P, r, \gamma \rangle$, where \mathcal{S} is the state space, and (a, z) , with $a \in \mathcal{A}_d$ and $z \in \mathcal{A}_c$, represents a hybrid action, $\gamma \in [0, 1]$ is the discount factor. At each step, the agent receives a reward $r(s, a, z, s') \in \mathbb{R}$ for performing an action (a, z) in state s and transitions to the next state s' with probability $P(s'|s, a, z)$. We wish to find the policies $\pi_d(a|s)$ and $\pi_c(z|s, a)$, which determine a discrete action and a corresponding continuous action, respectively, for each state, to maximize the expected sum of discounted rewards, i.e., the return $R = \sum_{t=0}^T \gamma^t r(s_t, a_t, z_t, s_{t+1})$, where T is the maximum time step in a finite-horizon setting.

E.1 PPO

To maximize the return, policy gradient methods are typically employed, directly improving a stochastic policy π_Φ using gradient ascent. A general policy gradient method aims to maximize the following objective:

$$\nabla_{\Phi} J(\Phi) = \mathbb{E}_{(s, a, s') \sim \pi} \left[\sum_{t=0}^T \nabla_{\Phi} \log \pi_{\Phi}(a_t | s_t) \mathbf{M}_t \right]$$

where \mathbf{M}_t represents any value-oriented metric that guides the action distribution output by the policy towards high-value regions. A widely used choice for \mathbf{M}_t is the advantage function $A(s_t, a_t)$, which can be estimated using Generalized Advantage Estimation (GAE) [32].

However, vanilla policy gradient methods do not constrain the extent of policy changes, which can lead to large updates and potential collapse in policy performance. To mitigate the risk of aggressive updates, PPO [33] constrains the new policy to remain close to the old one by incorporating a clipped policy ratio $r(\Phi)$ within the objective, forming the surrogate objective $\mathcal{L}^{\text{surr}}$, defined as:

$$\mathcal{L}^{\text{surr}}(\Phi) = \mathbb{E}_{\pi} [\min(r(\Phi)A(s, a), \text{clip}(r(\Phi), 1 - \epsilon, 1 + \epsilon)A(s, a))],$$

$$r(\Phi) = \frac{\pi_{\Phi}(a|s)}{\pi_{\Phi_{\text{old}}}(a|s)}$$

To encourage adequate exploration during training, an entropy regularizer is applied, promoting the policy to try diverse actions. This leads to the entropy-regularized PPO surrogate objective \mathcal{L}^{PPO} :

$$\mathcal{L}^{\text{PPO}}(\Phi) = \mathcal{L}^{\text{surr}}(\Phi) + \mathbb{E}_{\pi} [\beta \mathcal{H}(\pi_{\Phi}(a|s))] \quad (10)$$

where β is the entropy bonus coefficient. While the actors are updated using \mathcal{L}^{PPO} to achieve higher returns, the critic is responsible for providing accurate state-value estimations, which are then used to compute the advantage function via GAE. The loss function for the critic, $\mathcal{L}^{\text{Critic}}$, commonly takes the form of Mean Squared Error

(MSE), is expressed as:

$$\mathcal{L}^{\text{Critic}}(\Psi) = \mathbb{E}_{\pi} [(V_{\Psi}(s_t) - R_t)^2], \quad R_t = \sum_{l=0}^{\infty} \gamma^l r_{t+l} \quad (11)$$

Notably, PPO can be applied to either discrete or continuous action spaces, but not simultaneously. For further implementation details, please refer to [12] and our code.

E.2 Hybrid Action Space and H-PPO

A hybrid action space commonly exhibits a hierarchical structure: a high-level discrete action is chosen first, followed by a low-level parameter, treated as a continuous action associated with the discrete action. H-PPO [4] is based on the actor-critic framework but enhances it by employing two parallel actors – one for selecting discrete actions and another for determining continuous actions – while a single critic estimates the state-value function.

The training schema of H-PPO is based on PPO, with the main difference being that the two actors are updated separately. Specifically, after sampling a batch of transitions (s, a, z, r, s') , the discrete actor is optimized by maximizing Eq. (10), denoted as $\mathcal{L}^{\text{PPO}}(\Phi_d)$, using (s, a, r, s') , whereas the continuous actor is optimized in the same form, denoted as $\mathcal{L}^{\text{PPO}}(\Phi_c)$, using (s, z, r, s') . Meanwhile, the critic is updated by minimizing Eq. (11), comparing its estimated state-values with the true return values based on (s, r, s') .

During evaluation, a state is first sent to the discrete actor and outputs an action probability distribution, from which a discrete action is sampled. The same state is subsequently sent to the continuous actor and outputs continuous parameters for each discrete action. The specific parameter corresponding to the selected discrete action is fetched, and a continuous action is sampled from a Gaussian distribution based on the selected parameter as the mean.

F PSEUDO-CODE

RELIEF comprises two trainable modules: the policy network Π_{ω} and the projection head g_{ϕ} . The policy network Π_{ω} includes l discrete and continuous actors, respectively, and a single critic. The actors represent sub-policies $\pi_{\Phi_{d,1}}, \dots, \pi_{\Phi_{d,l}}$ and $\pi_{\Phi_{c,1}}, \dots, \pi_{\Phi_{c,l}}$, while the critic represents the state-value function $V_{\Psi}(s)$. Thus, the training parameters are $\Phi_{d,1}, \dots, \Phi_{d,l}, \Phi_{c,1}, \dots, \Phi_{c,l}, \Psi, \phi$. For simplicity, we use ω to denote the parameters of all the actors and the critic. The pseudo-code for training RELIEF, which alternates between training the policy network and the projection head, is presented in Algorithm 1. The operations in line 5 and line 20 can be batchified by consuming a batch of graphs.

The implementation of bootstrap sampling in line 2 follows LEEP [7], which samples from the entire training dataset to generate overlapping sets of training contexts, providing l contexts for l sub-policies. Random sampling for each training context can satisfy the overlapping requirement, but may exclude some nodes. In few-shot scenarios with limited labeled graphs, omitting any sample is inefficient. Therefore, we first assign $\lceil m/l \rceil$ samples to each context without intersection, treating them as respective contexts for each sub-policy, where m is the number of graphs in the entire training set, and $\lceil \cdot \rceil$ denotes the floor function. We then randomly sample $[o \cdot \lceil m/l \rceil]$ graphs from all other contexts and append them, where

Algorithm 1: Training RELIEF

Input: The frozen pre-trained GNN model f_θ , training graphs $\mathcal{D} = \{(\mathcal{G}_1, y_1), \dots, (\mathcal{G}_m, y_m)\}$ corresponding to node numbers $\{n_1, \dots, n_m\}$, the number of sub-policies l , the maximum number of nodes N , the number of times the projection head is trained per epoch q , and the maximum training epoch E .

Output: Optimal policy network Π_ω and projection head g_ϕ .

- 1: Initialize parameters ω and ϕ ;
- 2: Bootstrap sampling l training graph sets $\{\mathcal{D}_1, \dots, \mathcal{D}_l\}$ from \mathcal{D} for l actors;
- 3: **for** epoch = 1 to E **do**
- 4: **for** $i = 1$ to l **do** ▷ Policy network training
- 5: **for each** (\mathcal{G}_j, y_j) in \mathcal{D}_i **do**
- 6: Compute initial loss $\mathcal{L}_0 = \mathcal{L}(g_\phi(f_\theta(\mathcal{G}_j)), y_j)$;
- 7: Initialize a prompt feature matrix \mathbf{P}_0 with zeros;
- 8: Initialize an experience replay buffer \mathcal{B} .
- 9: **for** $t = 1$ to n_i **do**
- 10: Construct state s_t by Eq. (1);
- 11: Determine a feature prompt $p_t^{a,z}$ by sub-policies $\pi_{\Phi_{d,i}}$ and $\pi_{\Phi_{c,i}}$ and adds to \mathbf{P}_{t-1} ;
- 12: Compute instant reward r_t by Eq. (2);
- 13: Save the transition $(s_t, a_t, z_t, r_t, s_{t+1})$ to \mathcal{B} ;
- 14: **end for**
- 15: Update discrete actor $\pi_{\Phi_{d,i}}$, continuous actor $\pi_{\Phi_{c,i}}$ and critic $V_\Psi(s)$ with \mathcal{B} by Eq. (4), Eq. (6) and $\mathcal{L}^{\text{Critic}}$;
- 16: **end for each**
- 17: **end for**
- 18:
- 19: Initialize an empty list \mathcal{D}^* ; ▷ Projection head training
- 20: **for each** (\mathcal{G}_k, y_k) in \mathcal{D} **do**
- 21: Initialize a prompt feature matrix \mathbf{P}_0 with zeros;
- 22: **for** $t = 1$ to n_k **do**
- 23: Determine a feature prompt $p_t^{a,z}$ by joint policies $\pi_{d,J}$ [Eq. (5)] and $\pi_{c,J}$ [Eq. (7)] and adds to \mathbf{P}_{t-1} ;
- 24: **end for**
- 25: Save the prompted graph \mathcal{G}_k^* to \mathcal{D}^* ;
- 26: **end for each**
- 27: **for** times = 1 to q **do**
- 28: Update the projection head with \mathcal{D}^* by Eq. (3);
- 29: **end for**
- 30: **end for**

o is the overlapping ratio, set to 0.2. This ensures each context overlaps with others while utilizing all training graphs.

Note that at the evaluation stage, the joint policies $\pi_{d,J}$ and $\pi_{c,J}$ are utilized to attach feature prompts, similar to the projection head training, so it is not further described here.

G COMPLEXITY ANALYSIS

We analyze the time complexity of training and evaluation RELIEF for one epoch. The GNN model is a L_g -layer GIN with a hidden size d_g . By neglecting the dimension discrepancy between actors and the critic, we assume that the policy network is equipped with $(2l + 1)$ L_p -layer MLPs with a hidden size d_p , where l is the number of sub-policies. The projection head is a L_h -layer MLP with a hidden size

d_h . In addition, N , E are the maximum number of nodes and edges of m and m' graphs in training and evaluation sets, respectively, and D is the initial dimension of node features.

G.1 Detailed Complexity

The training process involves agent sampling, policy network training and projection head training.

Agent sampling. As we discuss in Section 3.2, the trainable components of actors and the critic are essentially MLPs. Starting with a pair of discrete and continuous actors, to determine prompt features at each step for one graph, the state with dimension d_g is passed to the two actors, with a complexity of $2O(d_g d_p + L_p d_p^2)$. The prompted graph is then sent to the GIN to obtain node representations, with a complexity of $O(L_g(Ed_g + NDd_g))$. Using mean pooling, the node representations are transformed into a graph representation, with a complexity of $O(Nd_g)$. Subsequently, by feeding these representations into the projection head, it outputs predictions with a complexity of $O(d_g d_h + L_h d_h^2)$, and computes the loss with $O(1)$. This process repeats N times to collect N transitions. Consequently, by sequentially performing sampling for each pair of actors and processing all m graphs in the training set, the total time complexity is:

$$mN \cdot [2O(d_g d_p + L_p d_p^2) + O(L_g(Ed_g + NDd_g) + Nd_g) + O(d_g d_h + L_h d_h^2) + O(1)] \quad (12)$$

Policy network training. A total of mN transitions are used for sequentially updating l pairs of actors, along with the critic. Therefore, the complexity of policy network training, which essentially updates MLPs, is:

$$3mN \cdot O(d_g d_p + L_p d_p^2) \quad (13)$$

Projection head training. This process is similar to agent sampling, except that it uses joint discrete and continuous policies to incorporate prompts. Then, the projection head is updated q times based on the prediction loss. Thus, the time complexity of projection head training is:

$$mNl \cdot [2O(d_g d_p + L_p d_p^2) + O(L_g(Ed_g + NDd_g) + Nd_g)] + mq \cdot [O(d_g d_h + L_h d_h^2) + O(1)] \quad (14)$$

To sum up, the time complexity of training one epoch is the sum of Eq. (12), Eq. (13) and Eq. (14).

The time complexity during the evaluation stage is similar to that of projection head training, since it also involves inserting prompts using joint policies, but making predictions with the projection head only once, rather than q times. Therefore, the time complexity of evaluation can be derived by replacing q with 1 and m with m' in Eq. (14).

G.2 Simplified Complexity

Given the cumbersome expression of time complexity, we aim to simplify and approximate it for clearer insight. Specifically, we unify all the hidden sizes d_g , d_p and d_h as d , and ignore small variables as constants, such as the number of layers $L_{(\cdot)}$ and training times q for the projection head. Then, the simplified time complexity of

training one epoch is:

$$m \cdot O(N^2 Dd + N^2 d + Nd^2 + NED + d^2 + N + 1)$$

and the simplified time complexity of evaluation is:

$$m' \cdot O(N^2 Dd + N^2 d + Nd^2 + NED + d^2 + 1)$$

Since the dimension D and d are fixed given specific application scenarios, the main bottleneck of the framework lies in $O(mN^2 Dd)$

and $O(mNED)$, indicating that the computation time will noticeably increase with the number of large graphs scaling up. Fortunately, the results in Section 5.2 demonstrate that RELIEF is data efficient, meaning that with a few samples, i.e., small m , RELIEF can already achieve desired performance. Furthermore, more efficient exploration methods can be applied to RELIEF to decrease the sampling cost, which is left for future work.

Received 20 February 2007; revised 12 March 2009; accepted 5 June 2009